SGP-TR-108

- Reservoir Technology - Geothermal Reservoir Engineering Research at Stanford

Principal Investigators:
H.J. Ramey, Jr., P. Kruger, Roland N. Horne,
F.G. Miller, W.E. Brigham

September 1986

Sixth Annual Report
Department of Energy Contract Number
DE-AS03-80SF11459
(DE-AT03-80SF11459)
For the Period
October 1, 1985 through September 30, 1986

Stanford Geothermal Program
Interdisciplinary Research in
Engineering and Earth Sciences
STANFORD UNIVERSITY
Stanford, California

TABLE OF CONTENTS

PREFACE

The Stanford Geothermal Program conducts interdisciplinary research and training in engineering and earth sciences. The central objective of the Program is to carry out research on geothermal reservoir engineering techniques useful to the geothermal industry. A parallel objective is the training of geothermal engineers and scientists fo? employment in the industry. The research is focused toward accelerated development of hydrothermal resources through the evaluation of fluid reserves, and the forecasting of field behavior with time. Injection technology is a research area receiving special attention. The Program is geared to maintain a balance between theoretical, laboratory, and matching field applications.

Technology transfer is an integral part of the Stanford Geothermal Program. Major activities include a Geothermal Reservoir Engineering Workshop held annually, and weekly Seminars held throughout the academic year. The Workshop has produced a series of Proceedings that are a prominent literature source on geothermal energy. The Program publishes technical reports on all of its research projects. Research findings are also presented at conferences and published in the literature.

Geothermal reservoir engineering research at Stanford has gained considerable breadth through the Program's international cooperative projects. There are research agreements with Italy, Mexico, New Zealand, and Turkey. These international projects provide a wide spectrum of field experience for Stanford researchers, and produce field data with which to develop and test new geothermal reservoir engineering techniques.

The Stanford Geothermal Program was initiated under grants from the National Science Foundation in 1972 and continued under contracts from the Energy Research and Development Administration and, since 1977, the Department of Energy. This publication is the Sixth Annual Report to the Department of Energy under contract

DE-AS03-80SF11459 (previously DE-AT03-80SF11459) which was initiated in fiscal year 1981. The report covers the period from October 1, 1985 through September 30, 1986. The Injection Technology activities are now separate from the Reservoir Technology activities and are presented in the Second Annual Report to the Department of Energy under contract DE-AS07-841D12529.

The successful completion of the Stanford Geothermal Program's objectives depends on significant help and support by members of federal agencies, the geothermal industry, national laboratories, and university programs. These are too many to acknowledge by name. The major financial contribution to the Program is the Department of Energy though its San Francisco and Idaho offices. We are most grateful for this support and for the continued cooperation and help we receive from the agency staff.

Henry J. Ramey, Jr.

Paul Kruger

Roland N. Home

Frank G. Miller

William E. Brigham

1. INTRODUCTION

The Stanford Geothermal Program in fiscal year 1986 was divided into several task areas, as defined in Department of Energy contract DE-AS03-80SF11459. Three of the task areas were carried out within the Petroleum Engineering Department, and one within the Civil Engineering Department.

Reservoir definition research at Stanford consists of well test analysis and bench-scale experiments. Well test analysis offers a rapid way to perform an initial assessment of geothermal systems. Well testing includes both single-well pressure drawdown and buildup testing, and multiple-well interference testing. The development of new well testing methods continued to receive major emphasis during the year. A balance between theoretical and experimental studies is sought. The goal is to develop new methods for observing reservoir and to test these in the field. Bench-scale experiments are performed to determine fundamental flow characteristics of fluids and to provide a balanced university based research.

Heat extraction from rock will determine the long-term response of geothermal reservoirs to development. The work in this task area involved a combination of physical and mathematical modeling of heat extraction from fractured geothermal reservoirs. Experiments have been carried out in a rechargeable laboratory reservoir with comparative testing of alternative modes of heat and fluid production. The results are leading to a useful mathematical method for early evaluation of the potential for heat extraction in newly developing geothermal resources.

International cooperative research at Stanford has field applications as its focus. Several formal and informal cooperative projects were active during the year. The main objective of Stanford's cooperative research is the application and testing of new and proven reservoir engineering technology using nonproprietary field data and geoth-

ermal wells made available by steam field operators world-wide. Stanford has two formal cooperative agreements with foreign agencies. These are the DOE-ENEL cooperation with Italy, and IIE-SGP cooperation with Mexico. Informal agreements exist with colleagues in New Zealand, Turkey, and elsewhere. The interaction between academic research and field applications has proved valuable to the research and training program.

An annual Workshop of Geothermal Reservoir Engineering has been held at Stanford since 1975. It is attended by 120-140 geothermal engineers, scientists, and developers from around the world. Weekly seminars on geothermal energy matters are held at Stanford throughout the academic year.

2. RESERVOIR DEFINITION.

The main objective in this task is development and testing of new pressure transient interpretation methods.

2.1 Multiple Well Interference Testing in the Ohaaki Geothermal Field.

J. D. Leaver, A. Sageev and H. J. Ramey, Jr.

Multiple interference tests were carried out in the Ohaaki geothermal field between 1979 and 1983. Data were collected for **periods** of up to 200 days per test using both wellhead mounted water level recorders and quartz crystal pressure gauges each with a resolution of about 100 Pa.

Analysis of the test results showed that early time data **up** to the minimum significant pressure level of 3 kPa failed to match the theoretical curves due to the effect of earth tides. Clipping techniques often exclude data which fall when the overall trend is a rise and hence earth tide oscillations are either filtered out or occur below the resolution of the gauge. Tests B3, B7, B9, B10, C3 exhibited this characteristic at early time. Table 2.1.1 shows a summary of results obtained from tests performed in this study.

Interaction with more than one hydrological heterogeneity was indicated in Tests B1, B9, C1 due to the deviation of data at late dimensionless time from the initial, matched curve. Tests B1 and B9 showed pressure support effects while Test C1 indicated contact with a second no-flow boundary. The lack of consistency in these late time trends precluded further analysis. It is possible to speculate that the pressure support seen in Tests B1 and B9 was caused by the presence of a two phase zone which later collapsed and therefore did not appear in Test C1.

TABLE 2.1.1
TRANSMISSIVITIES AND STORATIVITIES
Multiple Well Interference Tests. Ohaaki Geothermal Field

TEST	OBS. WELL	SOURCE WELL	INTERWELL DISTANCE (m)	r_2/r_1	kh (d–m)	$\phi c_1 h$ $m/kPax10^4$)
B1	23	13	279	9.25	94	0.65
B2	23	13	279			2.50
B3	23	19	357	2.80	115	4.40
B4	23	13	279			
B6	23	20	411			
B7	34	31	564	1.80	49	15.00
B8	34	23	795			40.00
B9	34	19	727			5.20
B10	23	13	279	9.25	64	2.80
C1	13	20	687	4.00	64	1.00
c2	23	20	411	4.00	96	1.30
c3	34	20	1145			1.70

The interference response of Test B4 was affected by gravity segregation, thermal, moving front and deposition effects associated with the injection of colder separated brine into the reservoir. It may be possible to normalize all these effects with the aid of a thermal simulator but this has not been attempted in this study.

Non-uniqueness problems in Tests B8, B9, C3 meant that no values of permeability were obtained for these tests but values of storativity which are less affected by the non-uniqueness problems were retained. Tests B9 and C3 were expected to show no-flow boundaries but the boundaries if present occurred at r_2/r_1 ratio's of less than two making detection improbable.

Reservoir Parameters

The principal results obtained were that the average test transmissivity was 80 *d–m* and the average storativity was 2.4 x 10^{-4} with both values having a range of about ±50% if the two high storativity values from Tests B7 and B8 are excluded. For a porosity of 20% and reservoir thickness of 700 meters the average test compressibility is 1.7×10^{-6} kPa^{-1} and the average test permeability is 114 md. The estimated compressibility agrees with that for brine at the average production temperature 263°C indicating that there are no mobile two phase zones in the field.

Interpretation of the superposed inference ellipses indicates that there is a NE-SW trending no-flow boundary near the extreme northern end of the productive area of the field (Figure 2.1.1).

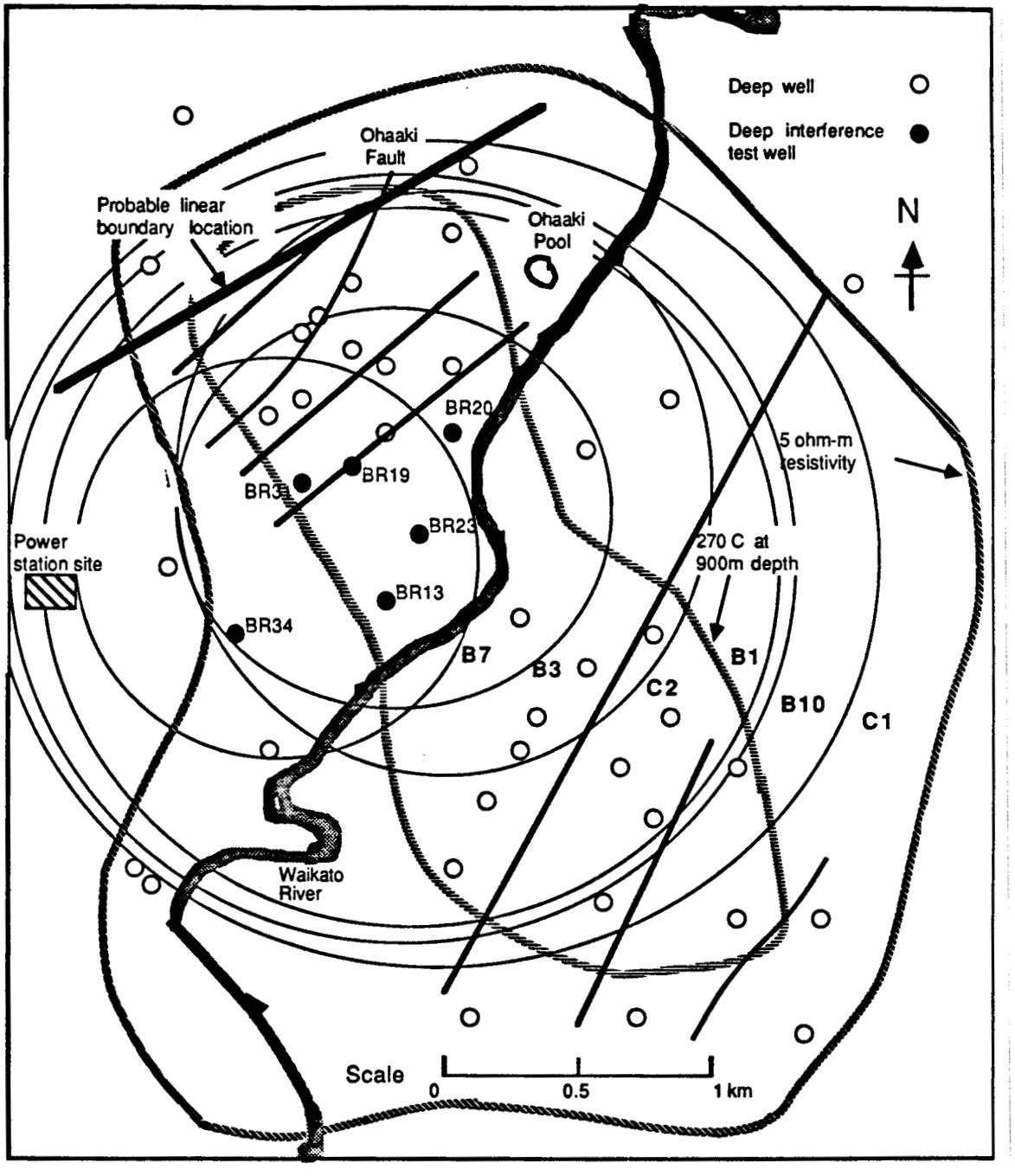

Fig. 2.1.1 Inference ellipse locations for Tests B1, B3, B7, B10, C1, and C2.

Conclusions

1. Careful interpretation is required to obtain the correct reservoir properties from interference tests.

2. The average permeability for the productive Ohaaki reservoir is about 110 md.

3. The average compressibility of $1.7 \times 10^{-6} kPa^{-1}$ derived from the interference tests indicates that there are no two phase zones in the Ohaaki reservoir within the sphere of influence of the test.

4. A no-flow boundary could be located utilizing the interference elipses deduced from 6 of the 12 tests analyzed.

5. Tests B1 and B9 showed evidence of late time pressure support which may have been due to a two phase zone in the reservoir which later collapsed, while Test C1 showed evidence of a second no-flow boundary.

A more detailed description of technics used for interpretation of data obtained from the multiple interference tests carried out in the Ohaaki geothermal field can be found in the following reference: Leaver, J.D., Sageev, A. and Ramey, J.J., Jr: "Multiple Interference Testing in the Ohaaki Geothermal Field" Paper SPE 15122, presented at the 56th California Regional Meeting of the Soc. of Petroleum Eng., held in *Oakland*, CA (April 2-4, 1986).

2.2 On Slug Tests Analysis in Double-Porosity Reservoirs

A. Sageev and H. J. Ramey, Jr.

The pressure response of a double-porosity reservoir to a slug test in a fully penetrating well with wellbore storage and skin is presented. Pseudo steady state matrix flow and transient matrix flow with and without skin are considered. Three kinds of type curves are discussed: early time log-log, intermediate time semi-log, and late time log-log. Pressure distribution around the active well and the prospects of interference slug testing are considered.

The early time response of the slug test depends on the presence of wellbore skin, hence, two kinds of early time type curves are presented. When the active well has wellbore skin, the early time correlating parameter is the product of the skin and the dimensionless storage, resulting in a new log-log type curve. When wellbore skin is not present, the early time response is proportional to the square root of time, with dimensionless storage as the correlating parameter. The intermediate time semilog type curves are applicable when wellbore skin is not present, or $C_D e^{2S} > 10^4$. The double porosity effects are significant in the late time log-log format, but the flat portion of the pressure response occurs at dimensionless pressures less than 0.01.

The radius of investigation of the slug test in a double-porosity system is also examined with and without wellbore skin at the active well. Interference responses and pressure profiles are presented. Although the presence of wellbore skin reduces the magnitude of the dimensionless pressure responses at observation wells, the detectabla radius of investigation does not significantly depend on wellbore skin. Interference slug testing in a double porosity system requires high precision pressure recording tools in the observation wells, since the double-porosity effects occur at small dimensionless pressures.

Transient matrix flow without matrix skin reduces the double-porosity effects, and limits the use of type curves for determining λ and ω. The slug test double-porosity effects in a reservoir with transient matrix flow with fracture skin and pseudo steady state matrix flow are similar.

Mathematical Considerations.

The derivation of the Laplace solution to the double-porosity slug test problem follows closely the derivation for the single-porosity system. In this report we will not present the derivation of the Laplace solutions. Instead, only the final solutions are presented. The wellbore Laplace solution **is:**

$$\bar{p}_{sD} = \frac{K_0\left(\sqrt{sf(s)}\right) + S\sqrt{sf(s)}K_1\left(\sqrt{sf(s)}\right)}{\frac{\sqrt{sf(s)}K_1\left(\sqrt{sf(s)}\right)}{c_D} + s\left[K_0\left(\sqrt{sf(s)}\right) + S\sqrt{sf(s)}K_1\left(\sqrt{sf(s)}\right)\right]} \tag{2.2.1}$$

where

$$f(s) = \frac{\omega(1-\omega)s+\lambda}{(1-\omega)s+\lambda} \tag{2.2.2}$$

and the dimensionless fracture storage parameter, ω, and the interporosity flow parameter, h, are:

$$\omega = \frac{(\phi Vc))_f}{(\phi Vc)_f+(\phi Vc)_m} \tag{2.2.3}$$

$$\lambda = \alpha \frac{k_m}{k_f} r_w^2 \tag{2.2.4}$$

The general Laplace solution of Equation (2.2.1) was used to generate the early time and late time limiting real time solutions.

Pressure Response

The late pressure characteristics of a double-porosity slug test are presented in Figure **2.2.1.** Curve **A** in Figure **2.2.1** is for a single-porosity reservoir with a dimensionless wellbore storage value of 10^4. Similar to all log-log curves for **a** slug test, the distinguishing portion of the curves occurs prior to $t_D/c_D = 10$. After this time, the single-porosity pressure responses join a **45** degrees straight line, observed by ***Ferris and Knowles*** **(1954).**

As we apply the slug test to a double-porosity system, two more parameters are added to the dimensionless storage, the fracture storage ratio, ω, and the interporosity flow coefficient, h. Curve B in Figure **2.2.1** presents a typical slug test pressure response in a double-porosity system, with $c_D = 10^2$, $\omega = 10^{-2}$, and $\lambda = 10^{-6}$.

Figure **2.2.2** presents several responses where $c_D/\omega = 10^6$ **and** $\lambda c_D = 10^{-3}$. Hence, all the responses start together with the single-porosity response at early time, then the curves deviate and separate from the single-porosity response. All the, double-porosity curves merge along the constant pressure flow period, and finally join the **45** degrees decline. The separation between the double-porosity curves is controlled by the parameter $\lambda c_D/\omega$ as will be discussed later.

The effects of the parameter λ are presented in Figure **2.2.3.** In this figure,, $c_D = 10^4$ and $\omega = 10^{-2}$, and λ varies between 10^{-6} and 10^{-9}. The smaller the value of h, the later the double-porosity effects occur.

The early time log-log pressure responses of Figure **2.2.2** are presented in Figure **2.2.4.** Here, $1 - p_D$ is graphed as **a** function of the dimensionless time over the dimensionless storage. The early time response represents the fracture system with the effective dimensionless storage of c_D/ω.

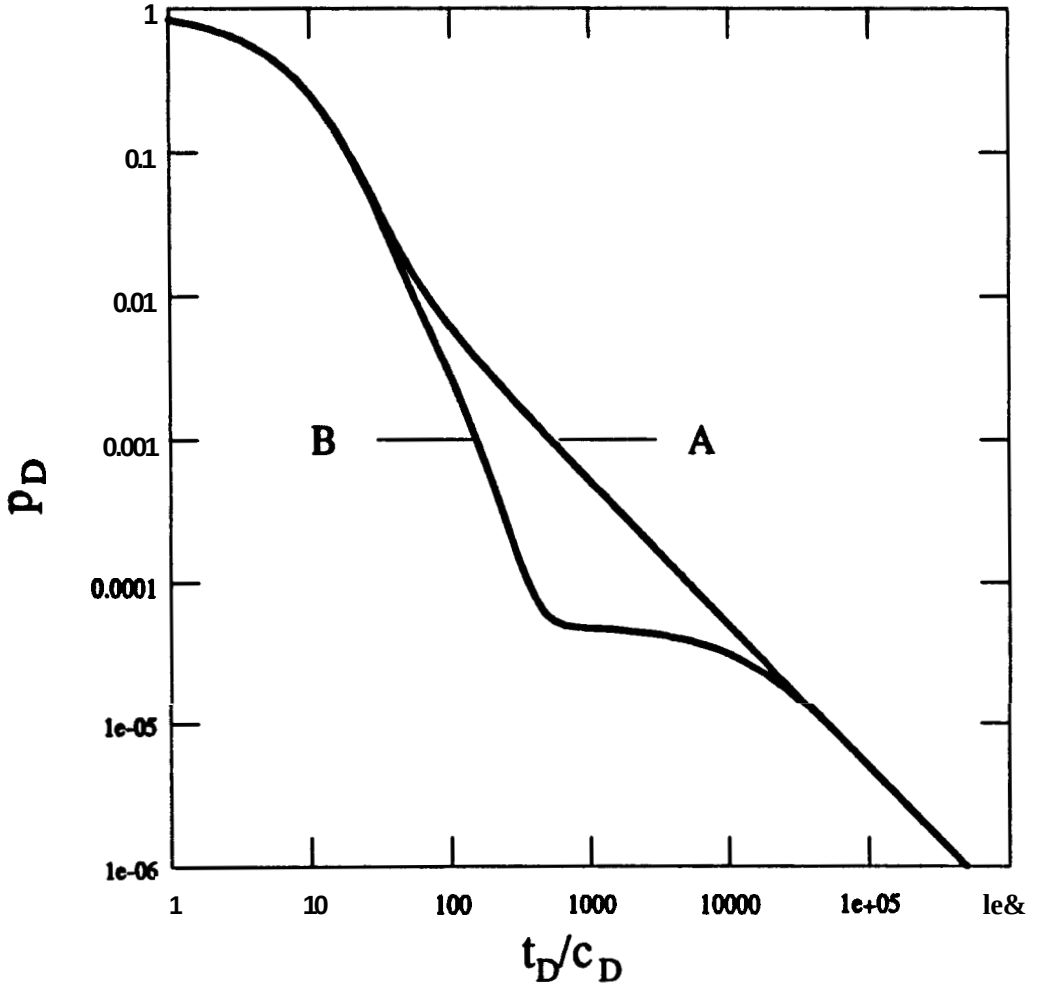

Fig. 2.2.1 A typical double-porosity slug test response. $c_D = 10^4$, s = 0. A: $\omega = 1$, $\lambda = 0$. B: $\omega = 10^{-2}$, $\lambda = 10^{-6}$.

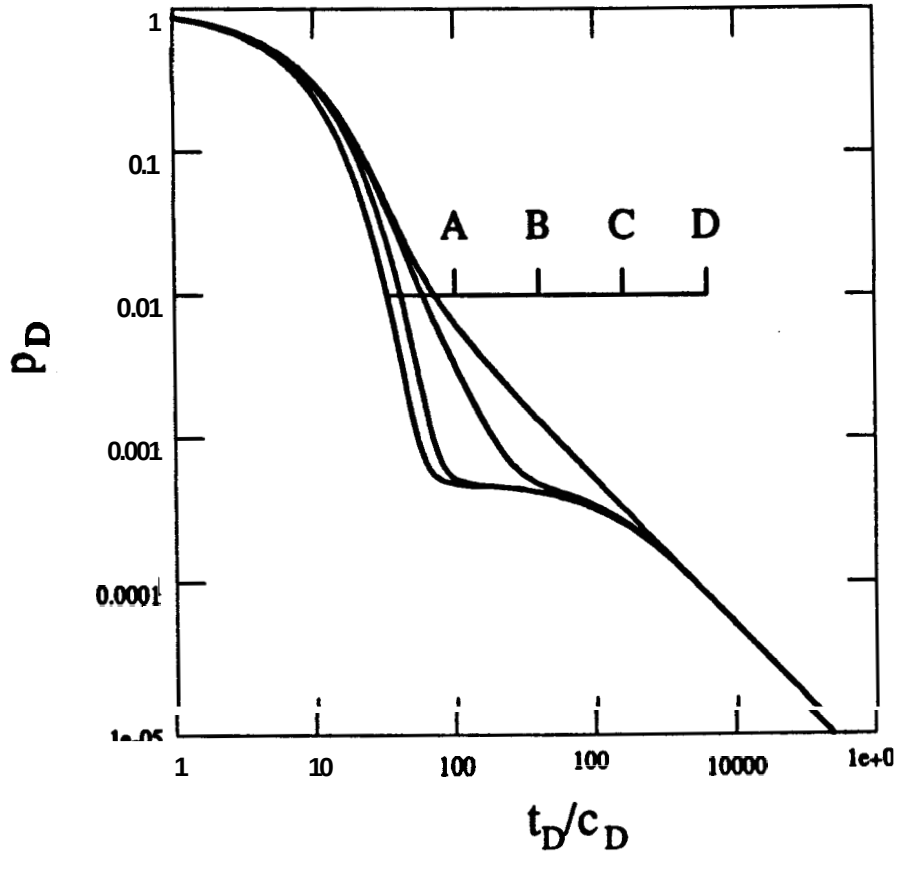

Fig. 2.2.2 Double-porosity responses with $c_D = 10^6$, $\lambda c_D = 10^{-3}$ and $s = 0$. A: $\omega = 1^{-3}$, $\lambda = 10^{-6}$. B: $\omega = 10^{-2}$, $\lambda = 10^{-7}$. C: $\omega = 10^{-1}$, $\lambda = 10^{-8}$, D: $\omega = 1$, $\lambda = 0$.

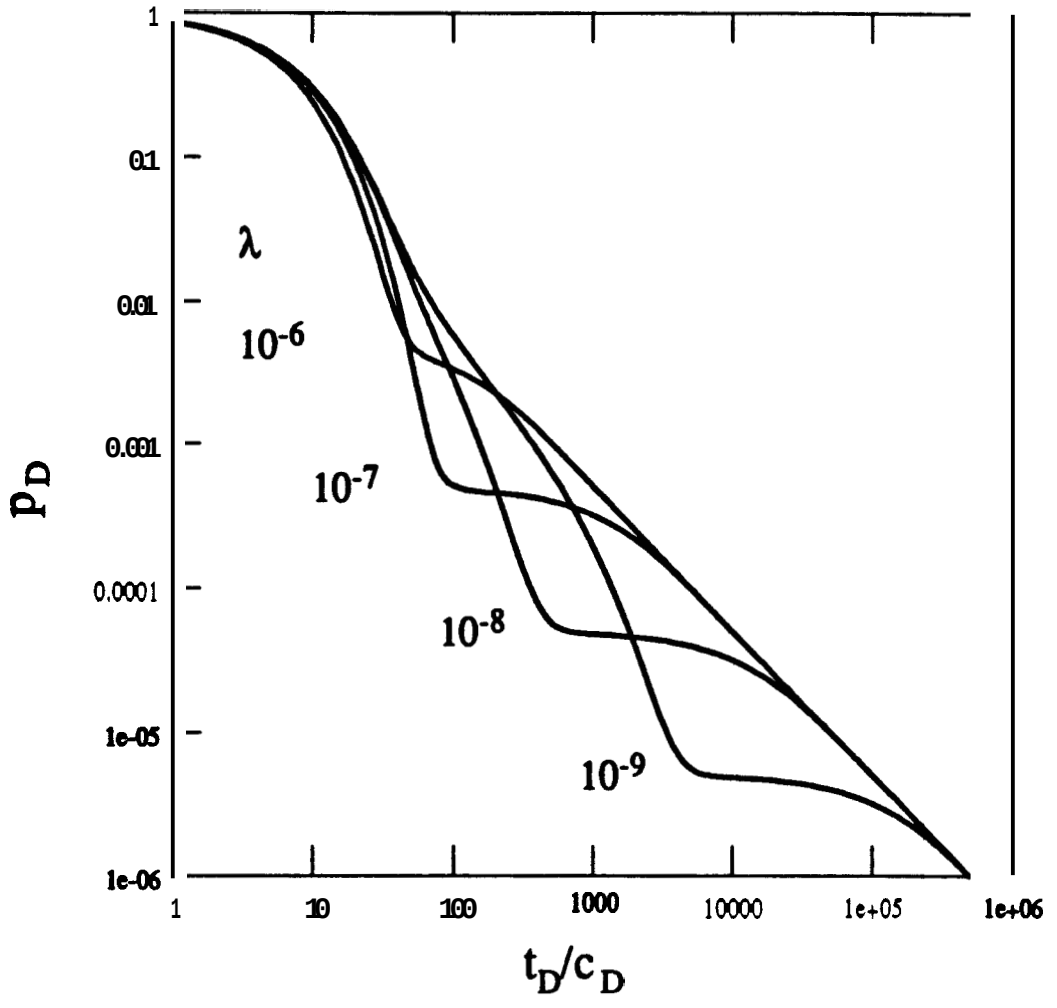

Fig. 2.2.3 Effect of λ on slug test early time log-log responses. $c_D = 10^{-4}$, $s = 0$, $\omega = 10^{-2}$, $\lambda = 10^{-6,7,8,9}$.

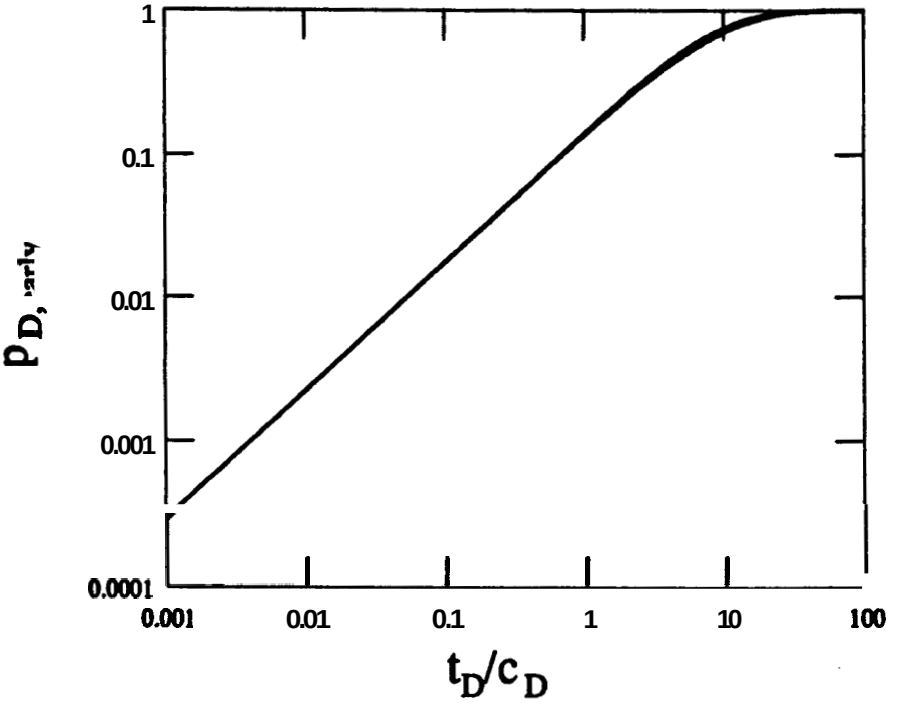

Fig. 2.2.4 Effect of λ on slug test late time log-log responses. $c_D = 10^{-4}$, $s = 0$, $\omega = 10^{-2}$.

The late time log-log double-porosity effects are summarized in a type curve presented in Figure **2.2.5.** This type curve is applicable for $\lambda c_D < 10^{-2}$. The four curves denoted by c_D/ω values are the single-porosity curves or the fracture flow dominated curves, presented by Ramey et al (1975). The region below the single-porosity pressure responses is mapped by two sets of curves. The five sloping curves represent the parameter $\lambda c_D/\omega$. These curves describe the acceleration of the pressure buildup in the well caused by fluid flowing from the matrix to the fracture in the near vicinity of the well. The horizontal lines represent the parameter λc_D. These curves describe the slowing down of the pressure rise in the wellbore caused by fluid flowing from the fractures to the **matrix** in the near vicinity of the well. Pressure profiles and interference responses are presented at the end of this section.

A hypothetical slug test response is presented on the type curve in Figure **2.2.5** as circles. From the early time match, the parameter c_D/ω is 10^6, and from the sharply declining match, the parameter $\lambda c_D/\omega$ is 10^{-2}. From these two parameters, the value of λ is determined, $\lambda = 10^{-8}$. Only if the pressure response displayed the transition to the constant pressure flow period, could the parameters c_D and ω be determined. This order of determination of the two double-porosity parameters is similar to the order in which λ and ω are determined from constant pressure and constant rate tests. In the example presented in Figure **2.2.5** the maximum value of the parameter λc_D is 10^{-3}. Hence, if we take this value for λc_D, the test parameters **are:** $c_D = 10^5$, $\lambda = 10^{-8}$, and $\omega = 10^{-1}$. If the pressure response continued to decline, and λc_D was 10^{-4}, the valuq of λ would remain 10^{-8}, but c_D and ω would be different, $c_D = 10^4$ and $\omega = 10^{-2}$.

For a more detailed description the reader should refer to the following publication: Sageev, A., and Ramey, H. J., Jr.: "On Slug Test Analysis in Double-Porosity Reservoirs", Paper SPE 15479 presented at the 61st Annual Technical Conference and

Exhibition of the Soc. of Petroleum Eng. **of AIME,** held in New Orleans, **LA** (Oct. 5-**8, 1986).**

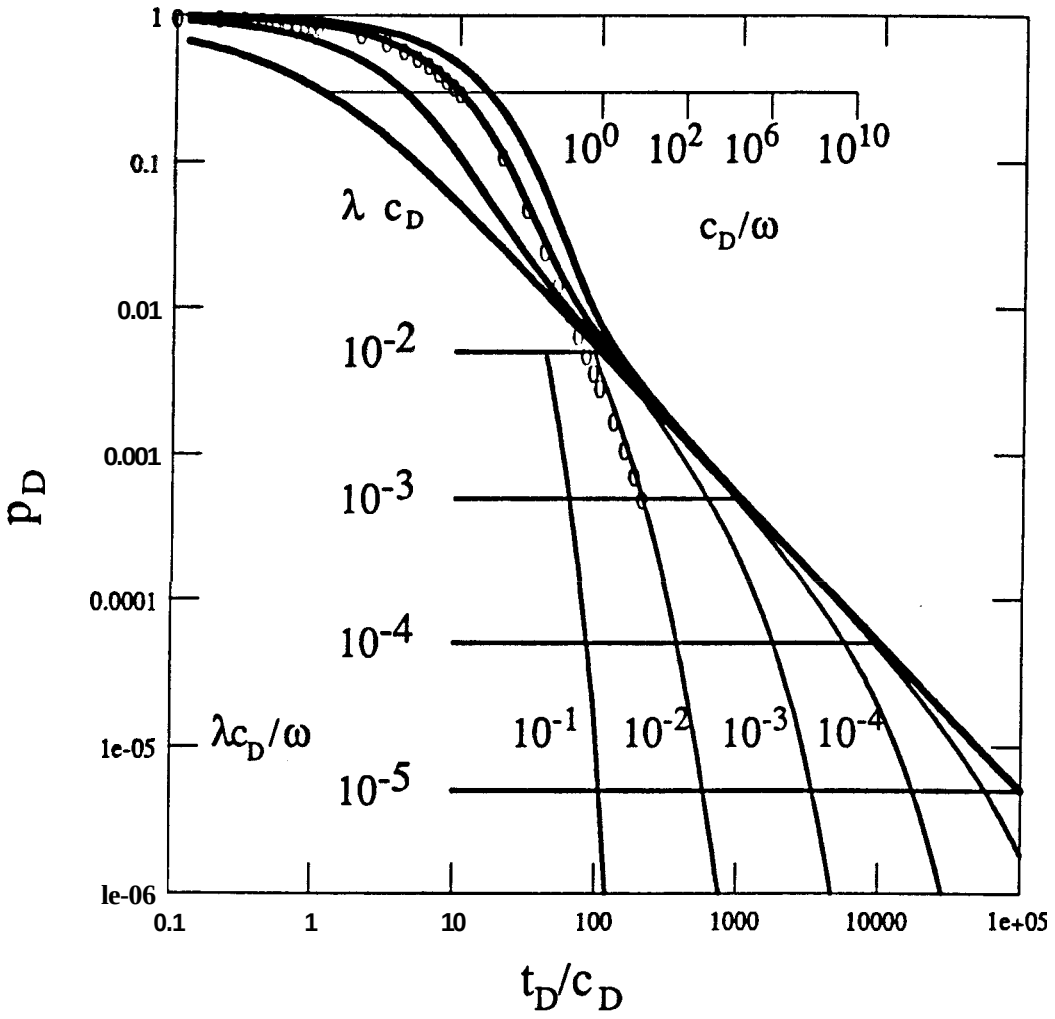

Fig. 2.2.5 Late time log-log type curve for double-porosity slug tests. $s = 0$.

2.3 Interference Testing: Detecting a Circular Impermeable or Compressible Subregion.

A. Sageev and R. N. Horne

A practical consideration of the effects of a single circular heterogeneous reservoir subregion on interference transient pressure testing is presented. The production well and the observation wells are external to the circular subregion. The internal circular boundary is considered as a constant pressure source or as an impermeable subregion. The constant pressure subregion has significant effects on interference pressure responses regardless of the size of the subregion. Ignoring the presence of a neighboring compressible portion of the reservoir, such as a gas or a steam cap, may yield erroneously high storativities and transmissivities. Multiple interference tests may suggest the probable location of the gas cap. The effects of an impermeable subregion are subtle, and in some cases large impermeable portions of the reservoir may not be detected by neighboring interference wells. Some interference tests in the presence of an impermeable subregion may yield high values of reservoir storativities, stemming from a pressure response similar in shape to the line source response. **A** map of the positions of interference wells that do not permit the detection of an impermeable subregion is presented.

Discussion of Results

A schematic diagram of the reservoir-well configuration is presented in Figure 2.3.1. Two dimensionless parameters are needed for this discussion. The dimensionless radius of the internal boudnary, F, is defined as:

$$F = a/r' \tag{2.3.1}$$

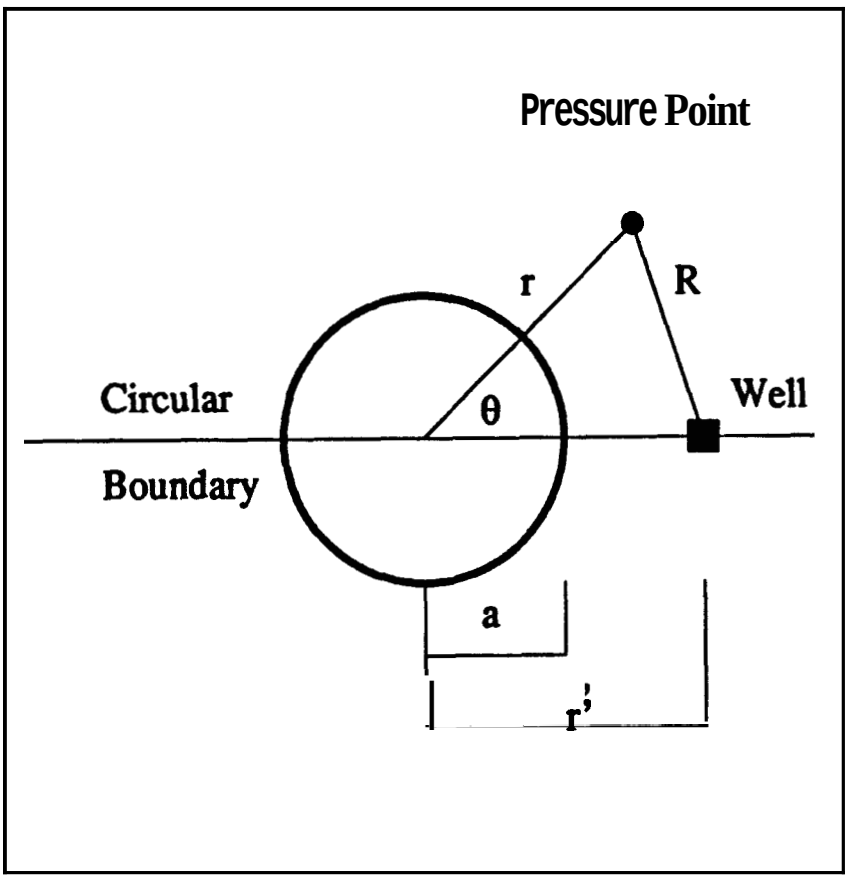

Fig. 2.3.1 A schematic diagram of wells near an internal circular boundary.

and the dimensionless radius between the center of the internal boundary and the observation point is defined as:

$$E = r/r' \tag{2.3.2}$$

Hence, the dimensionless radius of the internal circular boundary may vary between 0 for a diminishing boundary, and 1, for an infinitely large boundary. The dimensionless raduis for the observation well may vary between F and infinity. The angle of rotation, 8, is measured between the symmetry line and the line between the center of the internal boundary and the observation well. Hence, only 8 values between 0 and 180 degrees are considered.

Figure **2.3.2** presents the location of an interference point **A,** located on the opposite side of the internal boundary, with $E = 0.9$, $F = 0.7$ and $\theta = 180\,Deg$. The pressure responses of the interference point **A** are presented in Figure **2.3.3.** The heavy curve represents the line source response, for a constant rate well in an infinite homogeneous reservoir. The curve denoted by **A** is for an impermeable boundary, and is below the line source curve. However, at late time, the log-log pressure response approaches the line source response. The lowermost curve denoted by **B** is for a constant pressure boundary, and is significantly lower than the line source curve, even at extremely early time. At late time, the pressure response of curve **B** approaches a steady state condition. The same data of Figure **2.3.3** are presented in Figure **2.3.4** in a semi-log format. The curve denoted by **A** for the impermeable boundary is lower than the line source response, but has the same late time slope. This constant difference between the line source curve and curve **A** can be treated as a late time skin. The late time skin is different from wellbore skin, since it does not exist at the beginning of the test, when the region near the wells expands into the production well.

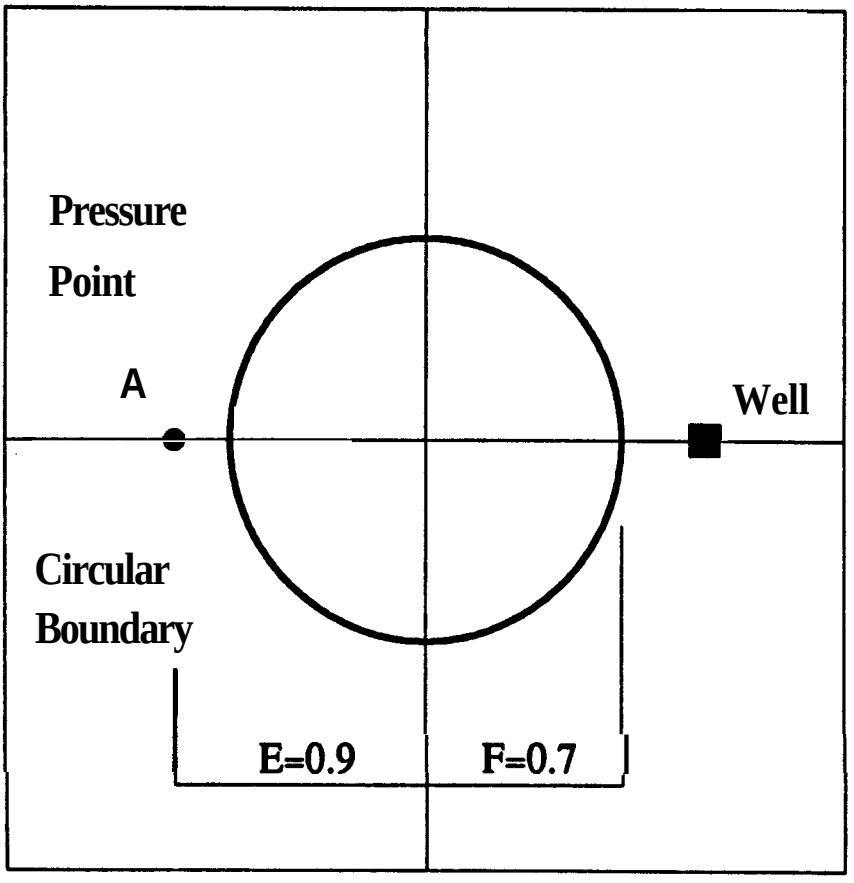

Fig. 2.3.2 **The location of an interference well with:** E=0.4, F=0.7 **and** ϕ=180°.

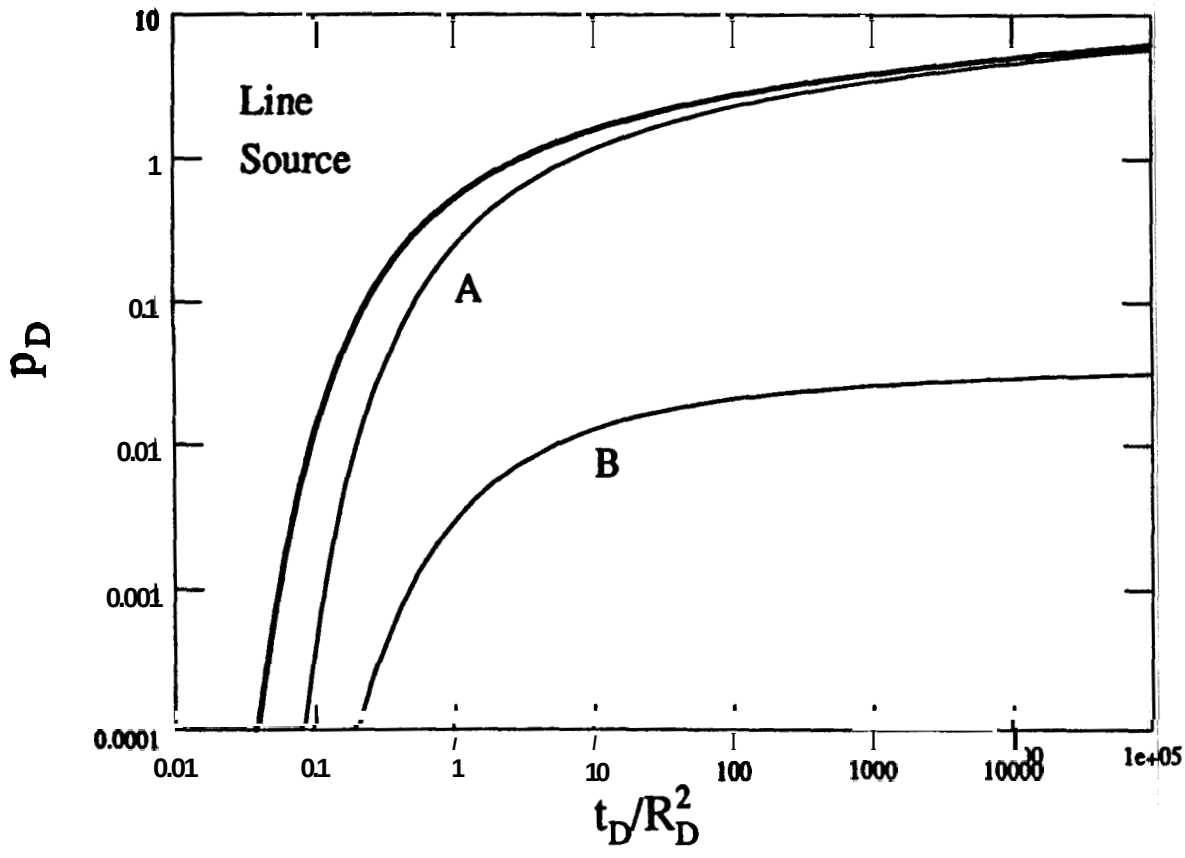

Fig. 2.3.3 Log-log interference pressure response near a constant pressure subregion: E=0.9, F=0.7 and ϕ=180°.

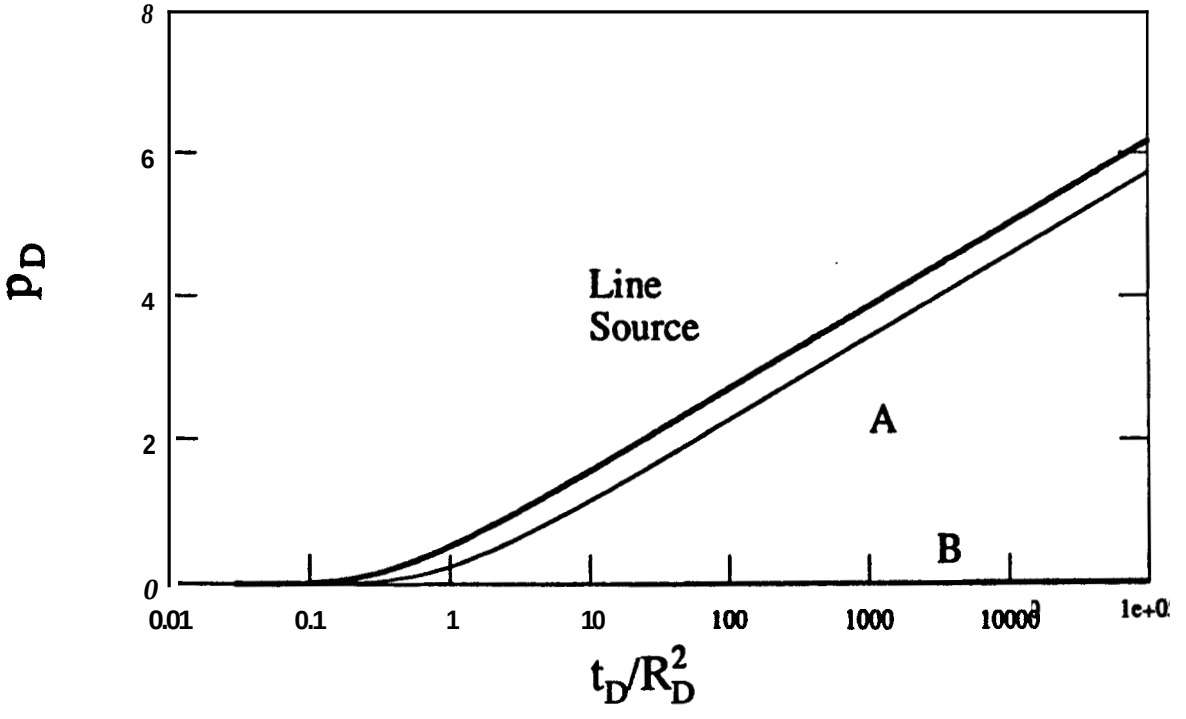

Fig. **2.3.4** Semilog interference response near a constant pressure subregion: E=0.9, F=0.7 and ϕ=180°.

At late time, the fluid in the reservoir near the wells and the internal boundary is flowing at a constant rate, coming from fluid expansion taking place away from the well-boundary region. The pressure response for the constant pressure boundary denoted by curve **B** is along to the dimensionless time axis.

Figure **2.3.5** presents the location of two observation wells denoted by **A** and **B,** and six different impermeable boundaries. The pressure response of observation well **A** to the six different boundary cases are presented in Figure **2.3.6.** All the six pressure responses are similar and match the line source response. The log-log match to the lnie source response has a positive result and a negative result. The positive result is that even if the semi-log straight line has not developed, the log-log analysis yields the correct storativity and transmissivity of the reservoir. The negative result is that although the interference well may be close to a large impermeable subregion, we have no indication of its existence. Figure **2.3.7** presents the same data of Figure **2.3.6** in a semi-log format. Even in the semi-log format, the curves are practically the same. The inset in Figure **2.3.7** shows the constant separation between the various curves, and the largest separation is for the largest impermeable boundary.

The presence of an impermeable subregion divides the reservoir into two parts. In once part the pressure drop is larger than the line source pressure drop, and the other **part** the pressure drop is smaller than the line source pressure drop. The separation line **has** the location:

$$x_D = Fa_D/2 \qquad (2.3.3)$$

where x_D is the dimensionless distance x/r_w along the symmetry axis from the center of the impermeable boundary in the direction of the production well. Figure **2.3.8** presents a suite of impermeable subregions with the separation lines between the two

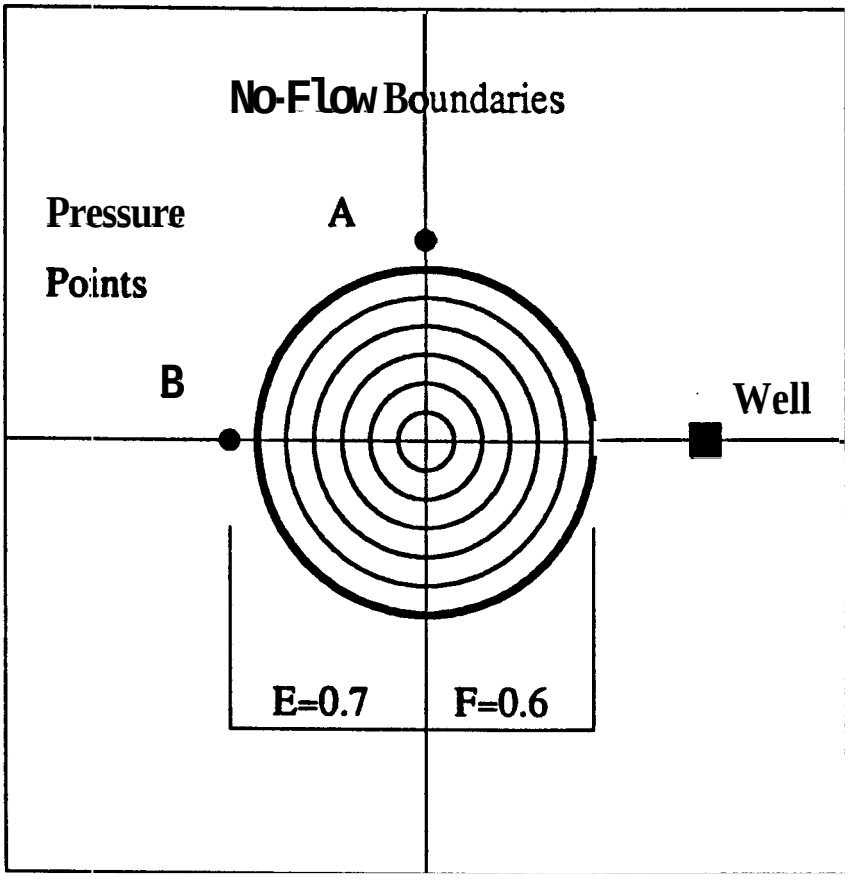

Fig. 2.3.5 The location of two interference wells: E=0.7, F=0.1, 0.2, 0.3, 0.4, 0.5, 0.6 and ϕ=90,180°.

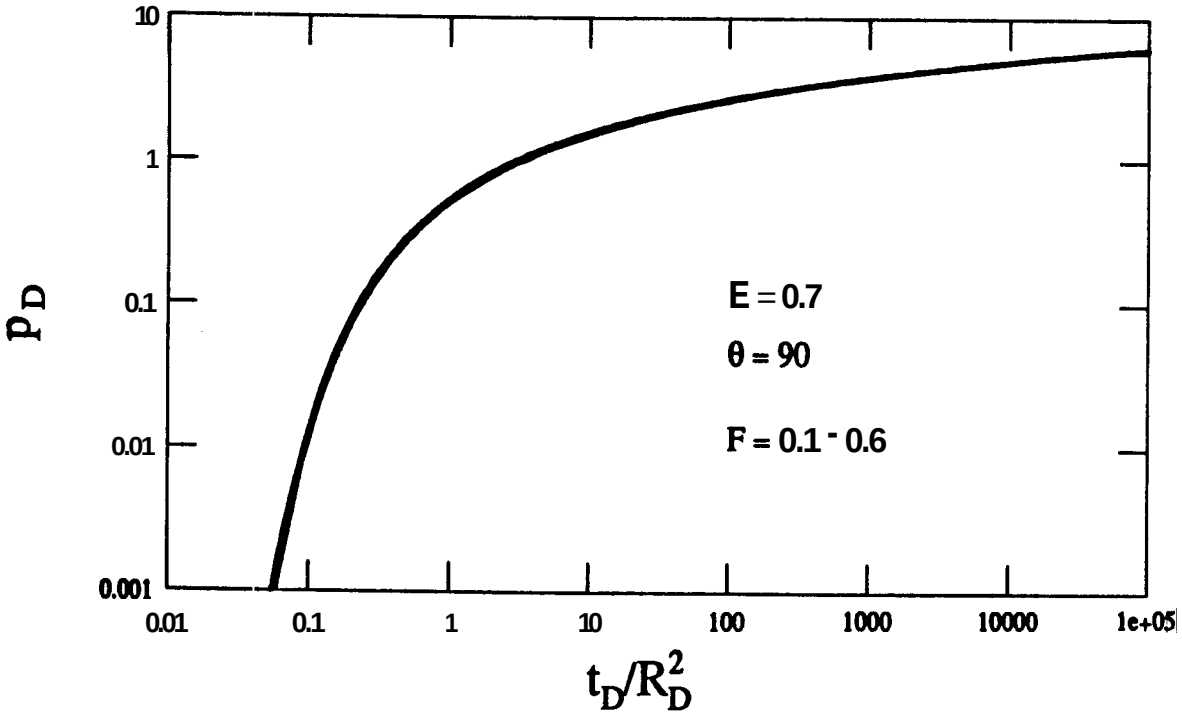

Fig. 2.3.6 **Log-log interference pressure responses near an** impermeable subregion: E=0.7, F=0.1, 0.2, 0.3, 0.4, 0.5, 0.6 and ϕ=90°.

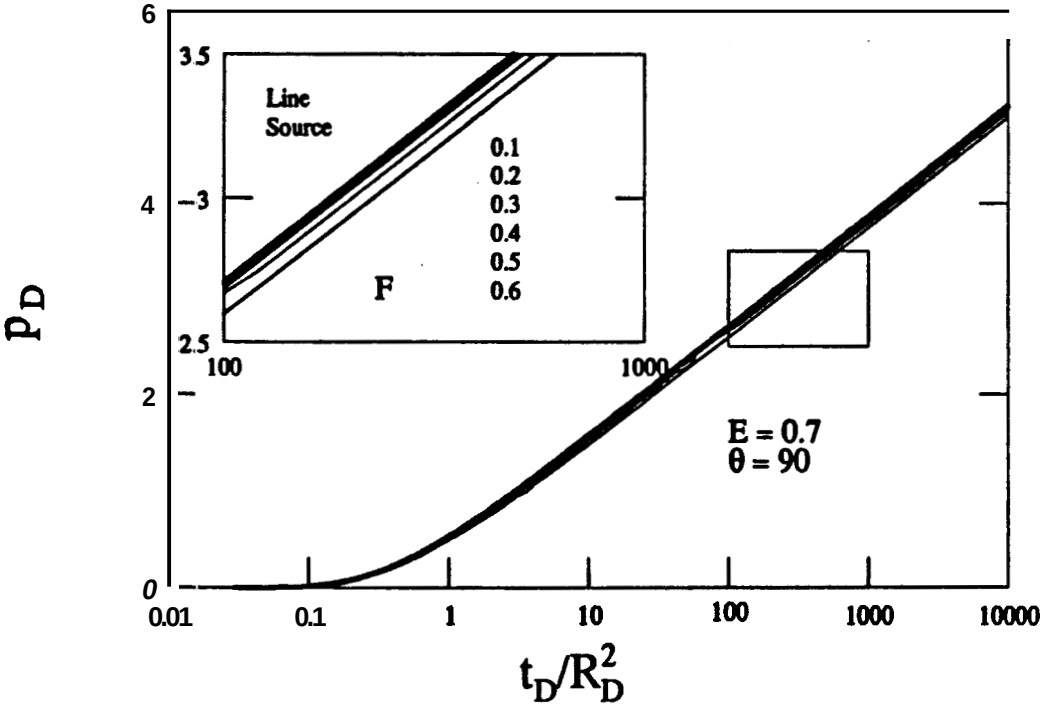

Fig. 2.3.7 Semi-log interference pressure responses near an impermeable subregion: E=0.7, F=0.1, 0.2, 0.3, 0.4, 0.5, 0.6 and ϕ=90°.

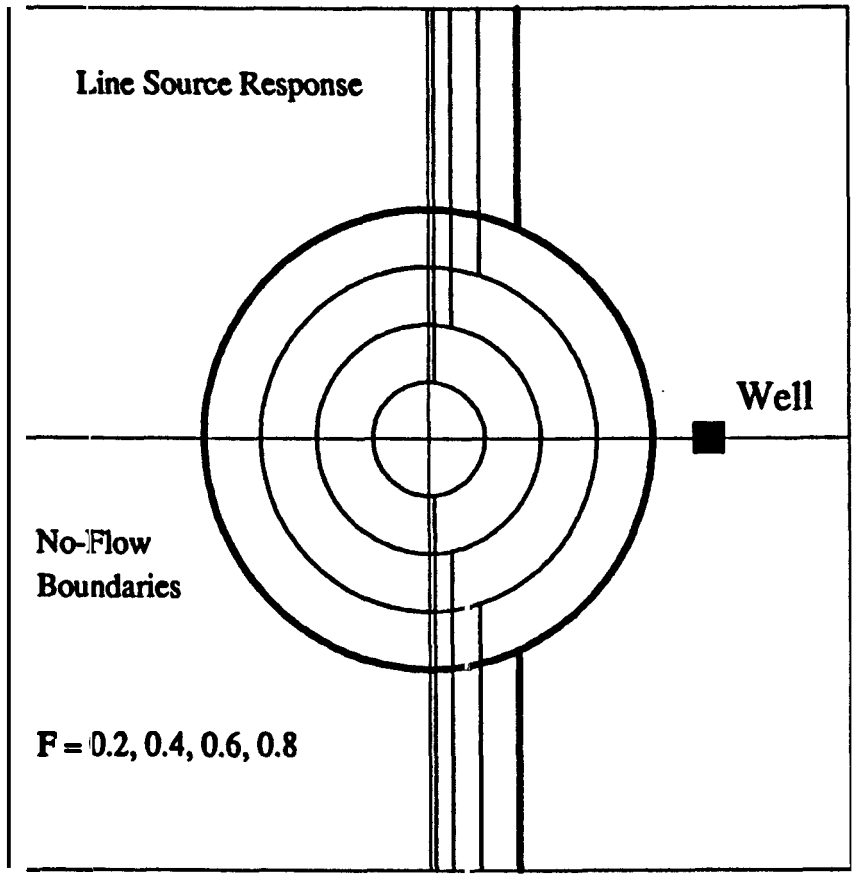

Fig. 2.3.8 The location of the separation lines for various sizes of impermeable subregions: F=0.7, 0.4, *0.6, 0.8.*

portions of the reservoir. Interference pressure responses of wells located along these lines or close to these lines (as can be seen in Figure 2.3.6) do not contain any indication of a large impermeable subregion near the production and observation wells.

A more detailed description of both mathematical development and analysis performed in this study can be found in the following reference: Sageev, A. and Home, R. N.: "Interference Testing: Detecting an Impermeable or Compressible Region", Paper SPE 15585 presented at the 61st Annual Technical Conference and Exhibition of the Soc. of Petroleum Eng. of AIME, held in New Orleans, LA (Oct. 5-8, 1986).

2.4 A New Type - Curve for Pressure Buildup Analysis with Boundary Effects

S. Mishra and H. J. Ramey, Jr.

For a well with wellbore storage and skin, producing from a bounded circular reservoir, it is possible for inner and outer boundary effects to interact and dominate the well pressure: response. Chen and Brigham **(1978)** investigated conditions under which such interference might obscure the semi-log straight line (corresponding ta infinite-acting radial flow) on a Horner buildup graph. It was found that this could occur even for small values of wellbore storage coefficient in reasonably sized drainage areas. However, they observed that a semi-log straight line with 5-10% error in slope could be found in almost all cases.

In this study, we expand upon the work of Chen and Brigham to identify conditions under which the inner and outer boundary combine to dominate the well pressure response. **A** second objective is to develop a general buildup type-curve incorporating inner and outer boundary effects.

In recent literature, use of the pressure derivative has been shown to enhance the pressure response signal (Bourdet et al., 1984). Hence pressure derivative is chosen as the variable of interest. The dimensionless buildup derivative group is defined as

$$\tilde{p}'_{Ds} = \frac{d(p_{DS})}{d(ln\Delta t_D)}$$

We examined the dimensionless buildup behavior for several combinations of c_D, S and r_{eD}. For large producing times, we found that two parameters are sufficient to correlate the buildup response when $\tilde{p}'_{Ds}$ is graphed as a function of $\Delta t_D/c_D$. Late-time data, influenced by outer boundary effects, are correlatable with r_{eD}^2/c_D.

Such behavior can be approximated by superposing the independent effects of a well with storage and skin in an infinite system and a well without wellbore storage and skin in a finite system. This is the basis of the type-curve shown in Fig. 2.4.1, where $\tilde{p}'_{Ds}$ is graphed against $\Delta t_D/c_D$ in log-log coordinates. The early and late-time correlating parameters are $c_{De}2S$ and r_{eD}^2/c_D respectively. The intermediate time period reflects the degree of interference between inner and outer boundary effects, which determines whether or not the semi-log straight line will develop on a pressure-time! graph.

The limits of the semi-log straight line may be specified by examining the behavior of $\tilde{p}'_{Ds}$ as it approaches (or deviates from) the value of 0.50 in Fig. 2.4.1. This indicates

$$\left.\frac{\Delta t_D}{C_D}\right|_{begin} \approx 30 \log C_D e^{2S}$$

$$\left.\frac{\Delta t_D}{C_D}\right|_{end} \approx \frac{r_{eD}^2}{100 C_D}$$

These equations are useful for test design as well as test interpretation, in identifying the proper semi-log straight line. The type-curve of Fig. 2.4.1 can also be used for this purpose in the usual manner.

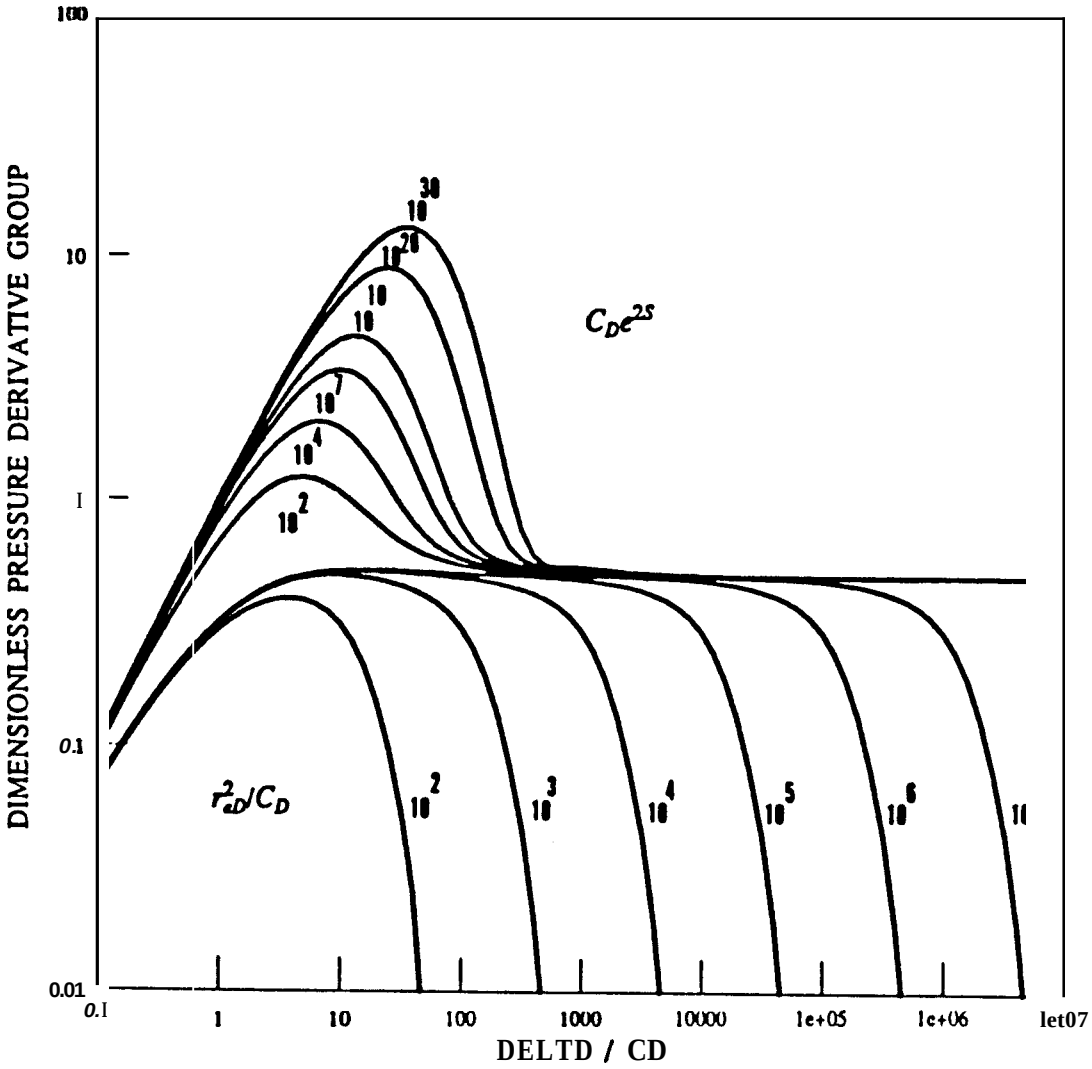

Fig. **2.4.1** Dimensionless pressure buildup derivative group vs. $\Delta t_D/c_D$. Early time behavior is correlated by the group c_De^{2S}, while late time data is correlated by the group r_{eD}^2/c_D.

2.5 Closed Chamber Well Testing

B. Salas and A. Sageev

Frictional effects were included in the closed chamber well test model developed by *Simmons* (1985) in order to develop a more general solution for the closed chamber well test.

Closed chamber well testing is used in the petroleum industry in the form of backsurge perforation cleaning *(Simmons* (1985), *Simmons* (1986)). As shown in Figure 2.5.1 the equipment used for backsurge operations includes the following: a work string composed of two remote controlled valves, a temporary packer, and a pressura recorder. The assembly is run into the wellbore with an enclosed chamber formed between the upper and the lower surge valves. The increase in the hydrostatic presi sure is recorded as the assembly is run into the well. When the packer is set the completion fluid overbalance is relieved, and the bottom hole pressure becomes equal td the static initial reservoir pressure. When the lower valve is opened the drawdown is, obtained, as the formation sandface is exposed to a minimum pressure, and fluids are produced. Then, the fluid level rises and the bottom hole pressure increases until it reaches the static reservoir pressure. Finally, the upper valve is opened, the packer released and the bottom hole pressure returns to an overbalance.

The closed chamber well test is similar to a conventional drillstem test; moreover, it is a generalized form of the drillstem test known as slug test. The closed chamber well test involves liquid level changes in the wellbore as a result of the instantaneous removal of a specific amount of liquid from the wellbore. The main difference between the closed chamber test and the slug test is wellbore storage. The slug test wellbore storage is constant, related either to fluid level rise or to fluid compression in a fixed volume. The closed chamber test wellbore storage varies from being controlled

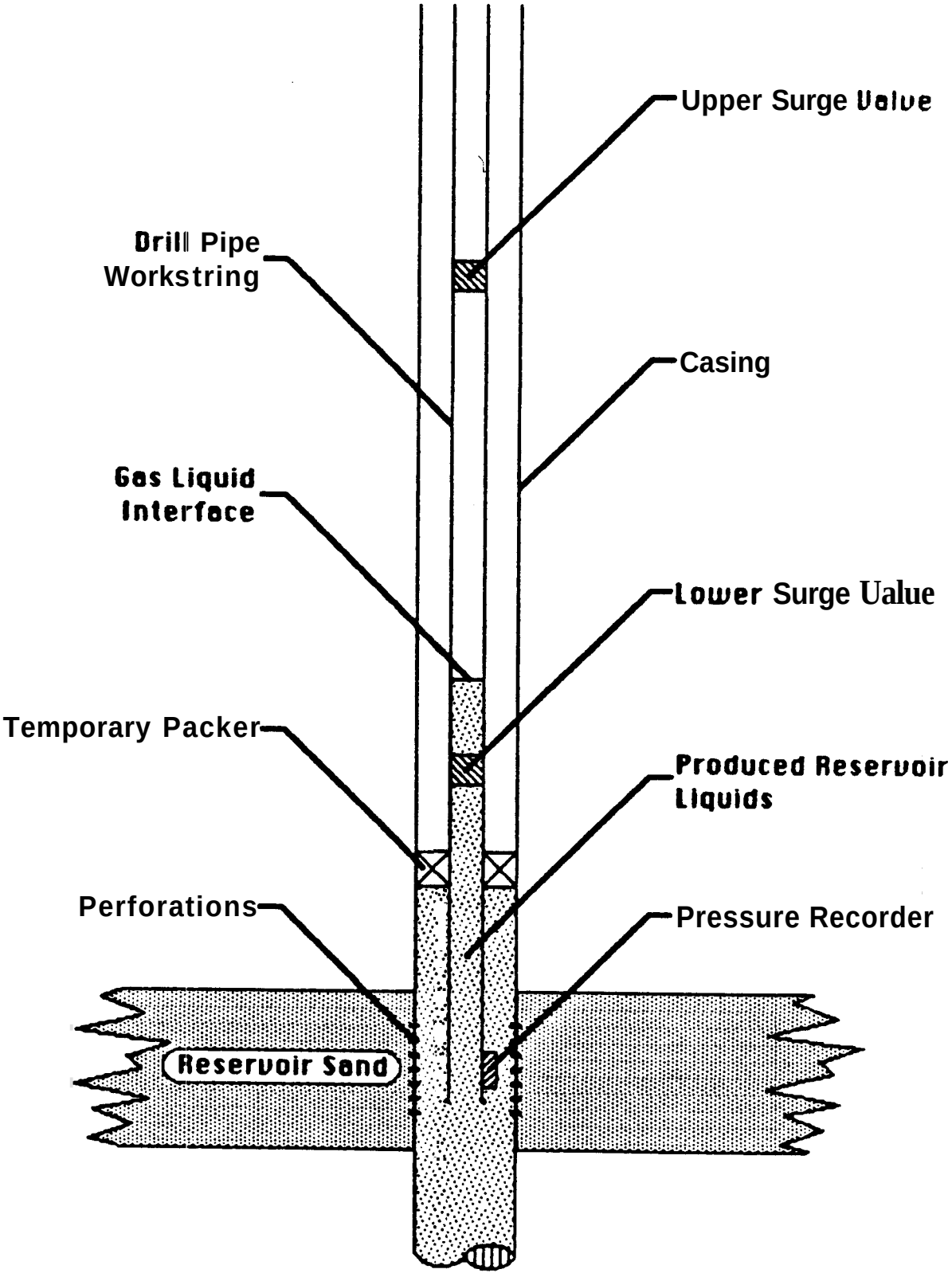

Fig. 2.5.1 Schematic representation of the closed chamber well test equipment.

by fluid level rise, to fluid compression in a changing volume. In a closed chamber test, the initial wellbore storage is high and reduces during the test, as the chamber gas compresses above the liquid column.

The variable wellbore storage and the presence of frictional and momentum effects throughout the test, make the closed chamber well test problem non-linear and difficult to solve analytically. Hence, numerical techniques are required to overcome the limitations and difficulties resulting from these non-linearities. Superposition of the cumulative influx, constant pressure solution of the radial diffusivity equation is used to overcome the limitations and difficulties resulting from solving the diffusivity equation in the presence of changing wellbore storage and frictional effects.

According to the results obtained, frictional effects significantly affect the early time pressure response, while late time pressure responses are not highly affected. Tha inclusion of tubing frictional losses in the closed chamber test acts like a choke, and reduces the instantaneous flowrate into the wellbore. However, at early time, when the bottom hole pressure is not affected by the pressure in the chamber, the presence of frictional effects increase the bottom hole pressure in comparison to the frictionless case. The gas compression in the chamber is only a function of the liquid level, (no mass transfer between the liquid column and the chamber gas). Since the flowrate is restricted by the tubing friction, the liquid levels are lower than in the frictionless case, and the rapid cornpression of the chamber gas is delayed. Hence, the late time bottom hole pressure for the friction case is lower than the bottom hole pressure for the frictionless case (Figure 2.5.2).

A sensitivity study was performed to analyze the influence of different tool and reservoir parameters on the closed chamber well test including frictional effects. The frictional pressure drop is closely related to the tool parameters like chamber diameter,

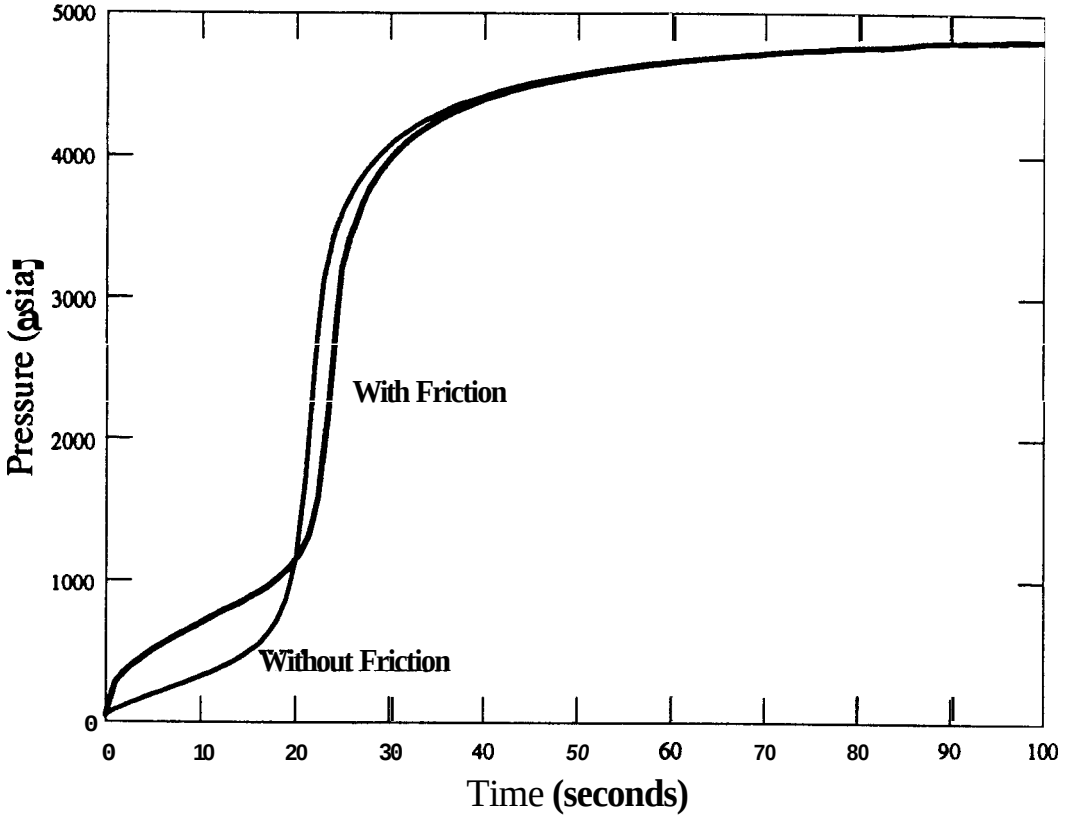

Fig. 2.5.2 Bottom hole pressure with and without friction.

absolute roughness and chamber length.

In general, the frictional pressure loss during a closed chamber test increases rapidly, levels off as it goes through a maximum, and finally decreases rapidly as the chamber gas compresses and chokes the well (Figure **2.5.3).**

The closed chamber well test model was improved by using variable time steps, hence, increasing the computation efficiency of the model. The program with variable time steps was also improved by including a restarting routine such that the program can be restarted from a given time greater than zero.

Momentum effects of the fluid between the lower valve and the formation, and in the cushion above the lower surge valve, were not considered in the model. Momentum effects are important in the cases where high flowrates occur and the initial fluid column in the wellbore must accelerate rapidly. For this reason it is recommended to include momentum effects on the closed chamber well test.

In developing the model, it is also assumed that wellbore liquids are incompressible. The late time response depends significantly on the high pressure compressibility of the gas. Yet, at these high pressures, the volume of the gas is small. On the other hand, the liquid column compressibility is low, but its volume is large. Wellbord storage is **a** function of the two fluid columns in the wellbore. Hence, future studies should analyze the influence of the produced liquid compressibility on the closed chamber pressure response.

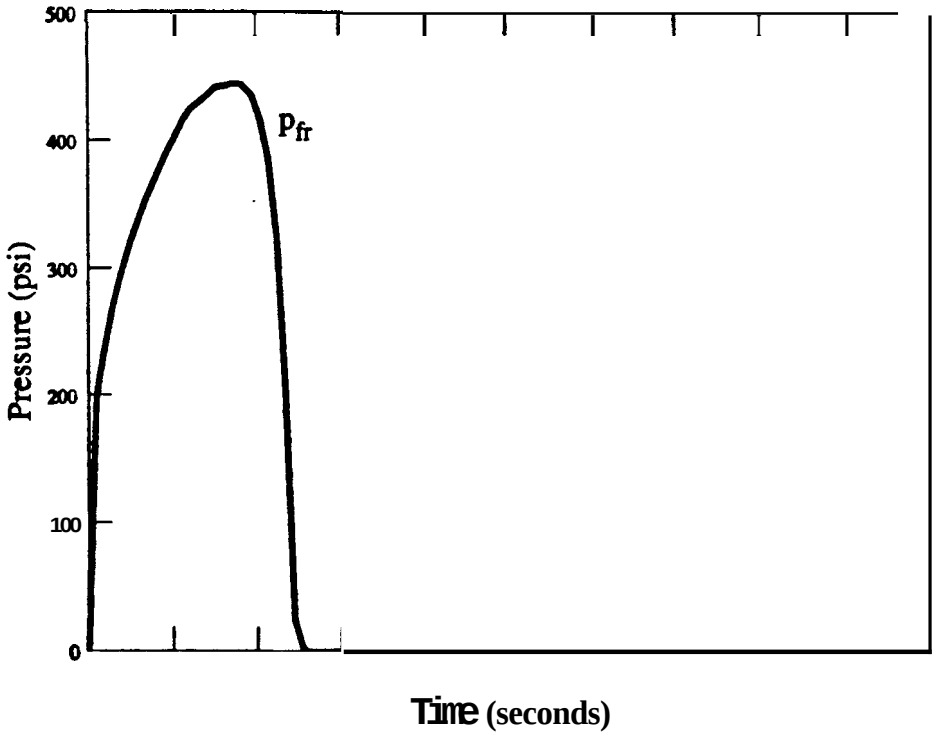

Fig. 2.5.3 Frictional pressure drop

2.6 Surface Adsorption in Geothermal Systems

J. Leutkehans, F. G. Miller and H. J. Ramey, Jr.

Surface adsorption has been an area of active research in a wide variety of disciplines. Several manifestations of this phenomenon are pertinent to the energy industry. This project focuses on the effects of adsorption in vapor-dominated geothermal reservoirs as well as in tight gas reservoirs.

Equipment alterations and maintenance accounted for a large portion of research time during this year. Work begun in the summer of 1985 to double the capacity of the high temperature bath was completed. As a precaution in case of diaphragm failure, additional pressure diaphragms were constructed, filled with oil, and connected to a vacuum pump to begin the outgassing process, Leak checks became part of a regular maintenance routine as well as inspection of valves and couplings. The couplings in particular were subject to failure, so stronger ones were made as replacements. Still, unresolved is the problem of a leak on one side of the oven system. The difficulty lies in the fact that it only occurs at high temperatures. One other major addition is an IBM Portable computer which will eventually control the data logging. At present, tha voltage ranges of the input signals are too diverse for one card to read. One solution may be to boost the weaker signal until the ranges are more compatible.

A new analysis program was developed based in part on the work of Hsieh, the previous researcher at Stanford. Though full testing awaits next fall, the program is designed to be simple to understand and use. Full documentation will facilitate any future changes if a more sophisticated analytical method is deemed necessary.

There were several new experimental runs completed during the year. To date, runs have been made on the following cores: 1) berea sandstone with three dead volume (DV) runs, four nitrogen (N2) runs, and one steam run at 150°C, two at 170°C

and one at 200°C, and **2)** Montiverdi **2** (Larderello, Italy) with five DV runs, three **N2** runs, and one steam run at 180°C, and **3)** Chuisdino **3** (Larderello, Italy) with two DV runs **and** one short **N2** run, and finally **4)** The Geysers graywacke with three DV runs, one **N2** run, and one steam run each at 150°C, 170°C, and **200°C.**

The adsorption isotherm for Montiverdi 2 for the nitrogen run is included as Fig., 2.6.1. The calculations used to generate this graph were done by hand as a first approximation and a check of part of the analysis program. The Z-factor was assumed to be equal to one, but in reality it is closer to 0.95. Thus, this analysis is slightly in error and will be corrected in the near future.

The goal for the immediate future is to put the program in working order and complete the analysis of the data already collected. Next fall quarter will be the time to reasses the project and determine the best **way** to move ahead.

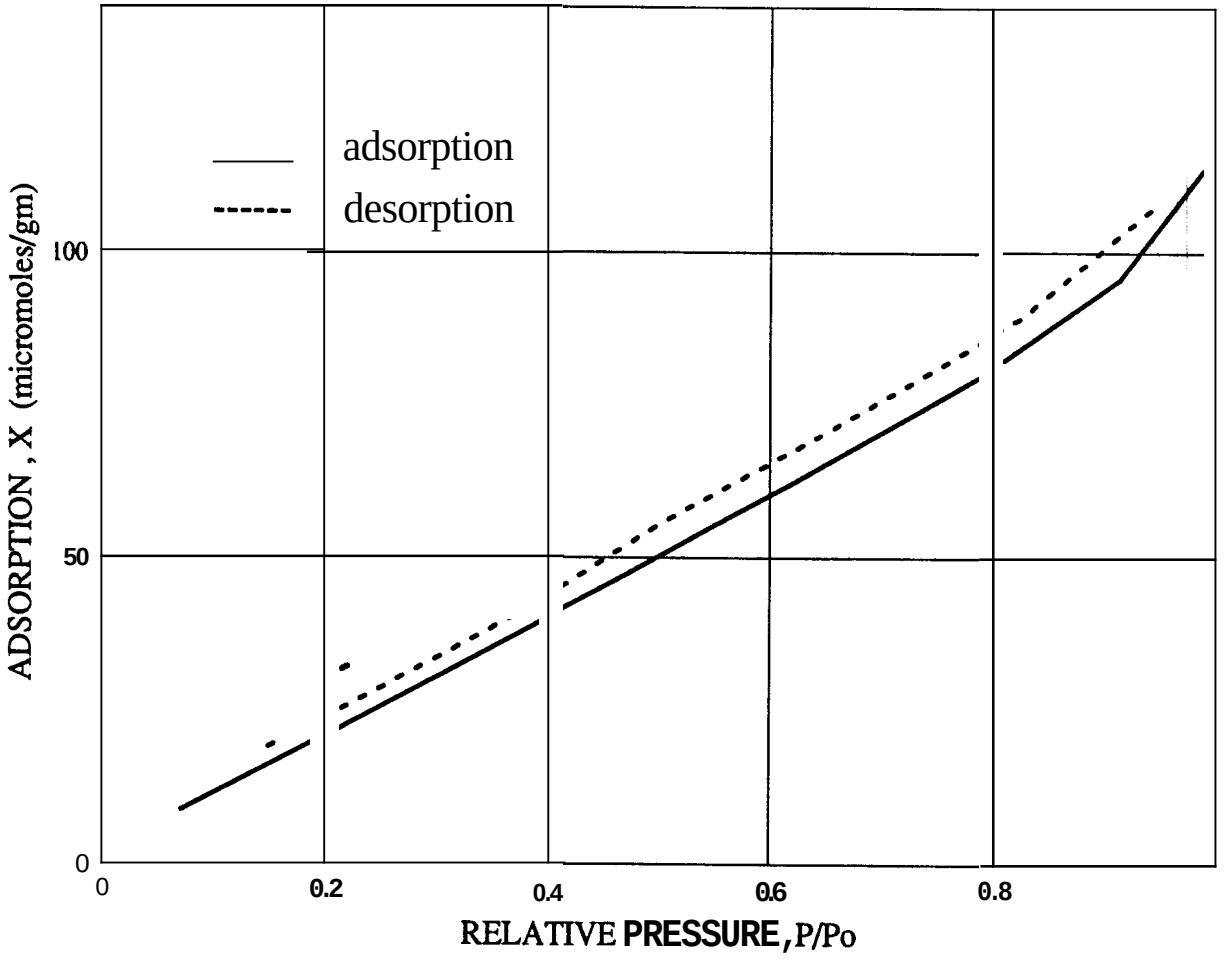

Fig. 2.6.1 Nitrogen adsorption isotherm for Montiverdi 2

3. HEAT EXTRACTION

S. Lam, A. Hunsbedt, R. Kruger and K. Pruess

During the current year, the heat extraction project continued research efforts directed mainly to four task areas: (1) completion of the SGP-LBL joint analysis of the SGP physical reservoir model experiments with the LBL reservoir simulator; **(2)** improvements in the one-dimensional Linear Heat Sweep model for analysis of recharge heat extraction in fractured hydrothermal reservoirs; **(3)** analysis of recharge heat sweep problems at the Cerro Prieto and Los Azufres geothermal fields in Mexico in cooperation with the Comision Federal de Electricided (CFE); and **(4)** completion of the design phase of the experimental study on thermal property changes in fractured hydrothermal reservoirs under recharge thermal stressing.

3.1 SGP-LBL Joint Study

During the contract year, several key milestones were reached. One of them was the completion of the cooperative reservoir model evaluation with Karsten Pruess using the LBL MULKOM/MINC simulator and the experimental data from the heat sweep experiments in the SGP Fractured-Reservoir Physical Model. The conclusion of this effort was that the LBL simulator did an excellent job of predicting the physical processes in physical model, especially under the very large thermal gradient conditions in the relatively small reservoir with complex boundary conditions. The results demonstrated the importance of specifying relevant parameters accurately to provide adequate modeling of the important physical processes. The joint report was prepared as a journal paper and submitted for archival publication(1).

(1) H. Lam, A. Hunsbedt, P. Kruger, and K. Pruess: "Analysis.....", submitted to J, Petro. Tech. **(1986).**

3.2 One-Dimensional Linear Heat Sweep Model

S. Lam and P. Kruger

A major effort during the year was the greatly expanded application of the SGF 1-D Heat Sweep Model in conjunction with data acquisition from the Comision Federal de Electricidad (CFE) under a long-standing program of cooperation sinca 1974. Table 3.2.1 shows the series of heat sweep analyses completed or underway with CFE.

Table 3.2.1
SGP-CFE HEAT SWEEP MODEL APPLICATIONS
September 30,1986

HSP	Field	Wells	Applications
0	Cerro Prieto	Western CPI	Cooldown Match
1	Los Azufres	Az31-Az26	Thermal Breakthrough
1b	Los Azufres	Az31-Az26	Sweep-Res. Fluid Mixing
2	Los Azufres	Az8-Az2	Recharge Return
3a	Los Azufres	Az15 Injector	Linear Heat Sweep
3b	Los Azufres	Az15 Injector	Radial Heat Sweep
4	Los Azufres	Tejamaniles	15 Prod - 4 Inj Wells
5	Los Humeros	Unit 1 H5-H7,H1	Directional Sweep
6	La Primavera	PR2-PR9	Dispersion Angle Sweep
7	Los Azufres	Az1-Az22	Unbounded Sweep
8	Los Azufres	Az14-Az4	Gravity vs Slant Sweep

The initial successes in the application of the 1-D Heat Sweep Model included a match of the modeled vs observed cooldown history at the western line of wells in the original Cerro Prieto I field during eleven years of production. The appropriate chemical and production data for the boundary wells and the next inner line of wells were provided by CFE. Analysis of reservoir temperature by geochemical thermometers yielded annually averaged mean cooldown rates for the two lines of wells, the boundary wells showing a greater rate of cooldown. Modification of the 1-D Heat Sweep Model allowed a matching of the observed cooldown curve at the boundary wells by a mixing model of sweep flow, distributed percolation from above, and reservoir fluid flow, each flow component at its respective temperature. The results of this heat sweep problem were reported at the 10th SGP Workshop (1985) and the 7th New Zealand Workshop (1985).

The program at Los Azufres accelerated during the year with progress on the first four heat sweep problems at both the vapor-dominated south zone and the two-phase north zone. HSP1 at the eastern border of the south zone was examined for heat sweep reinjection breakthrough from injection well Az31 to production well Az26. The very rapid expected cooldown (less than 10 years for 100% sweep flow) resulted in a revised problem, HSP1b, with the ratio of sweep flow to reservoir flow as the main parameter and variable effective reservoir fluid cooldown rate as a second parameter. HSP3 at the north zone was examined to estimate premature cooldown from recharge sweep flow from injection well Az15 across three newly drilled production wells towards the current production zone of four wells supplying the three north zone 5-MW wellhead generators. The heat sweep was examined as a comparison of cooldown expectations over a range of linear flow area (HSP3a) and radial dispersion angle (HSP3b). Figure 3.2.1 shows the heat sweep data for HSP3a,b as an example of the

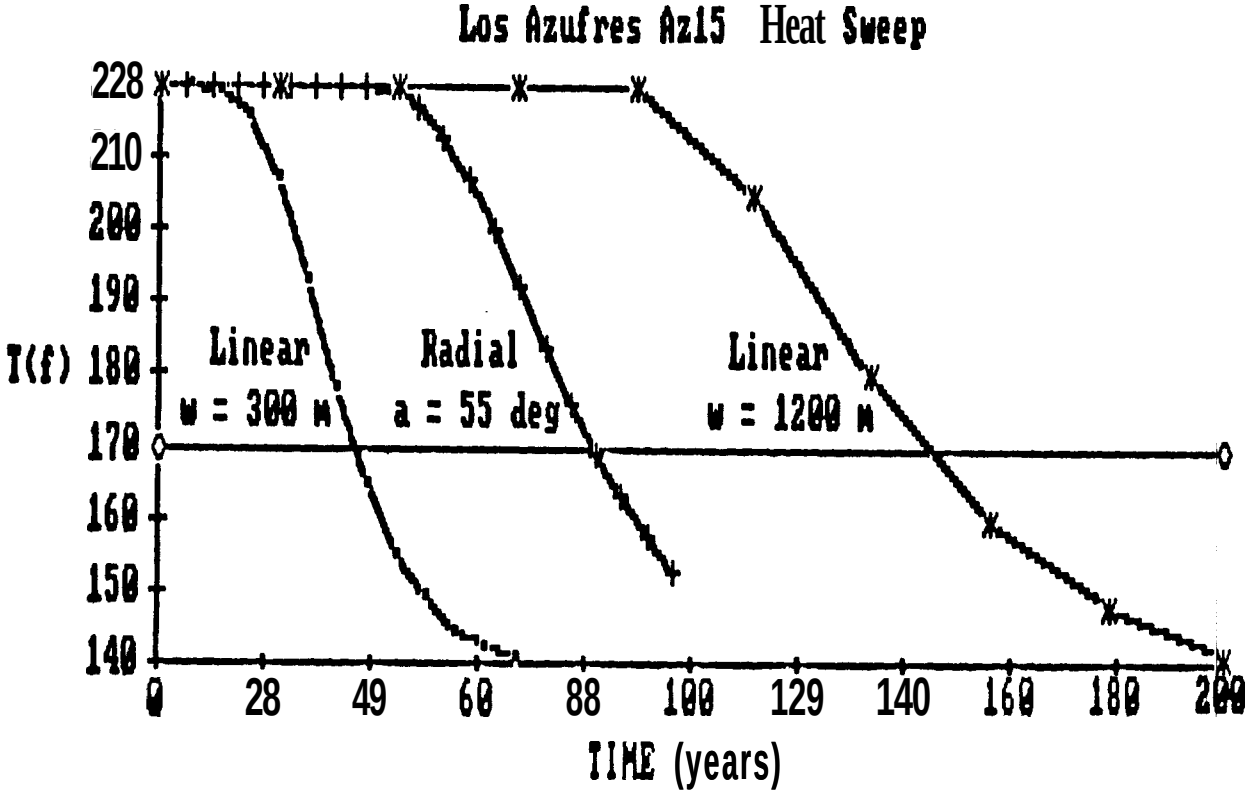

Fig. 3.2.1 **Comparison** of the fluid temperature cooldown curves for two linear widths and dispersion angle to cover the three newly drilled wells.

graphical output of the 1-D Heat Sweep Model. The results of these two Los Azufres applications are sufficient timely and are being reported at the 8th New Zealand Workshop (1986).

HSP2 at the western border of the south zone was of interest as a case of reinjection into well Az2 at a considerably lower depth (1000 m) than the production well Az8. For a variety of flow geometry assumptions, thermal breakthrough times in excess of one century helped explain why no tracer recovery was observed in the reservoir tracer flow test carried out in these wells.

HSP4 is an interesting problem involving a multiwell production - injection system for the 55-MW central power plant, purchased from the Baca Demonstration Project. The system comprises a reservoir field of 15 production wells and 4 injection wells. The problem was formulated as a matrix sweep problem using a weighting function for each injector-producer well pair. The heat sweep data for the 19 wells are being compiled by CFE.

During the year, with the announcement by CFE that 10 additional *5-MW* wellhead generators will be installed at Los Azufres and two new geothermal fields, additional heat sweep problems were formulated to help evaluate the contemplated reinjection plans for these new sites. These include HSP5 for ther pair of production wells H7 and H1 from reinjection well H5 at Unit 1 of the Los Humeros field in Puebla, and HSP6 for the pair PR2-PR9 at the La Primavera field near Guadalajara. The new well sites at Los Azufres include HSP7 for the well pair Az1-Az22 in the south zone and HSP8 for Az14-Az4 in the north zone. The results of the heat sweep analysis for the two new fields are being prepared for presentation at the 12th SGP Workshop in Janu*ary,* 1987 as a joint report.

The joint project with the Los Azufres operating staff was continued to examine the total body of chemical and production data from the wells supplying the original five wellhead generators to asses the extent of small drawdown on a potentially large resource resulted in a compilation of the first four years of production. A statistical analysis of the range of observed changes in these wells is being prepared for presentation at the 12th SGP Workshop as a joint report (1987).

3.3 Thermal Stress Effects on Thermal Conductivity

S. Lamb and P. Kruger

During the contract year progress was achieved in the study of the potential for change in productivity of geothermal reservoirs through changes in thermal conductivity in reservoir rock due to thermal stresses from cold-water recharge sweep. The model of thermal stress effects on thermal conductivity due to rapid large temperature change was completed by Stephen Lam for his PhD dissertation and all supplies for the experimental measurements program in the SGP Physical Reservoir Model have been acquired. Two granitic blocks with distributed thermocouples will be tested in the reservoir model to complete this phase of the project.

3.4 Activable Tracers

C. Chrysikopoulos and P. Kruger

During the contract year, efforts were successfully concluded on evaluating the thermal stability and adsorption properties of indium, chelated with EDTA and NTA to provide high sensitivity for enhanced reservoir tracer testing. Earlier efforts had shown that indium, among a group of four activable tracers suitable as high precision tracers in geothermal fluids, was the most promising for neutron activation and gainma-ray spectroscopy measurement. The chelated form was selected as the best means to enhance solubility in the difficult high-temperature rock-fluid geothermal environment, but uncertainty existed about its thermal stability and persistence in geothermal reservoirs during the life of a tracer flow test.

The chelated tracers, InEDTA and InNTA, were exposed to geothermal reservoir temperatures ranging from 150 to 240 C in special gold-lined vessels (provided by the USGS, Menlo Park) to remove material interferences in the thermal stability tests. Ex-

perimental stability data were obtained by activating samples in the 2 ug Cf-252 neutron source (provided by the Stanford Linear Accelerator Center). The experimental results were shown in Figures 3.4.1 and 3.4.2. The data indicate that indium, chelated with EDTA, could be thermally stable in geothermal reservoirs at temperatures up to about 200°C for at least 20 days.

The tracer was also tested for adsorption non-conservation by interaction with ground graywacke sandstones, typical of rocks in geothermal reservoirs. The resulting data are shown in Figure 3.4.3. The data indicate that the chelated form of indium is chemically stable, even in the presence of iron with a stronger EDTA chelate formation constant, and that the time limit on its use is influenced essentially by thermal degradation.

The data and conclusions of these experiments underwent Technology Transfer by means of (1) presentation at the 11th SGP Workshop on Geothermal Reservior Engineering*; **(2)** the Engineer Thesis of Costas Chrysikopoulos**; and (3) a SGP Technical Report***. The latter manuscript has been condensed and submitted for achival publication.

Other activities included the contact with the Cornwall Hot Dry Rock group in England to assist with the interpretation of the first application of indium EDTA-chelated activable tracer in a geothermal reservoir tracer test. The experiment was run in May, 1986 and the samples were shipped to the Harwell National Laboratories for neutron activation and radiation measurement. It is anticipated that the results of the Comwall experiment will be made available to the U.S. geothermal community.

Further analysis was made of the potential for a field laboratory facility using a mobile neutron generator and radiation detection eqiupment or on-site measurement.

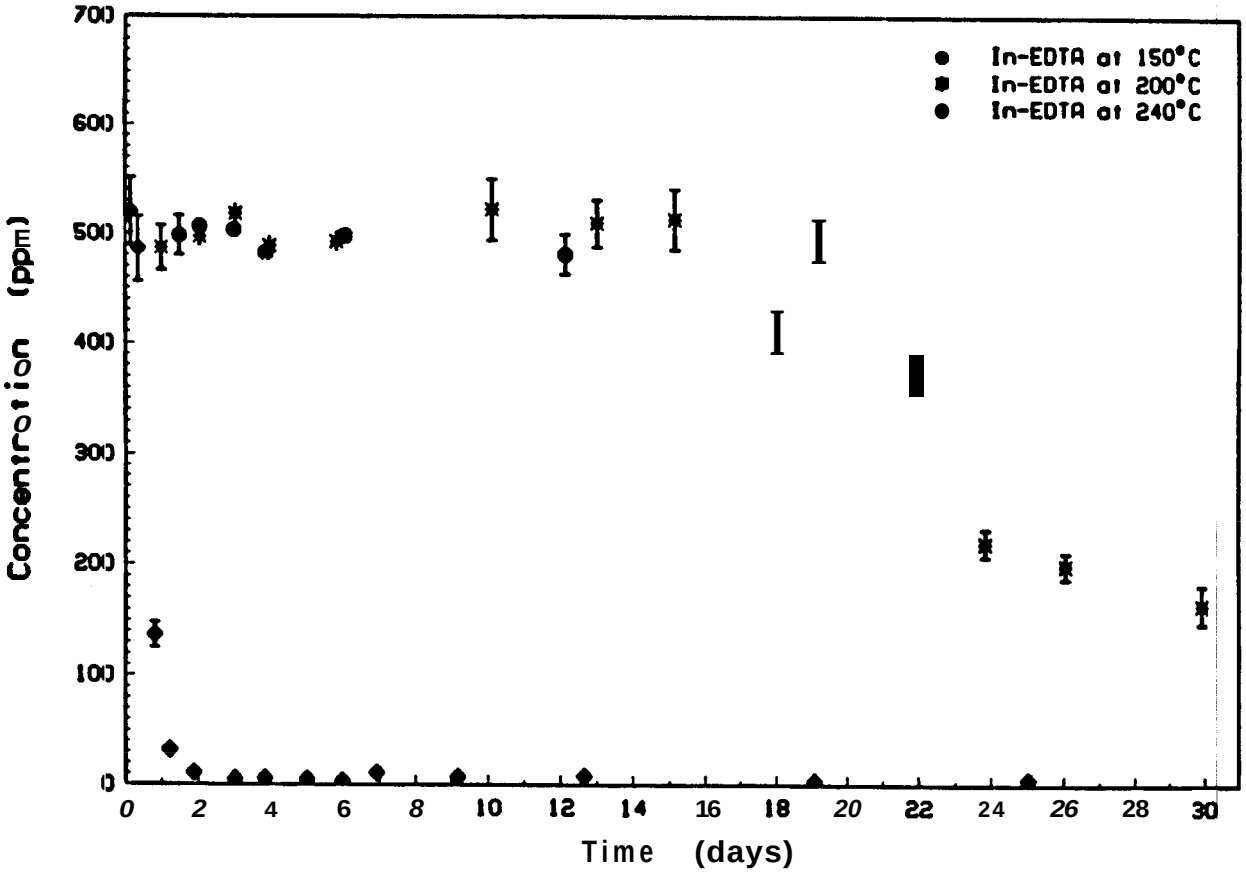

Fig. 3.4.1 Effect of temperature **and** time **on** InEDTA stability,

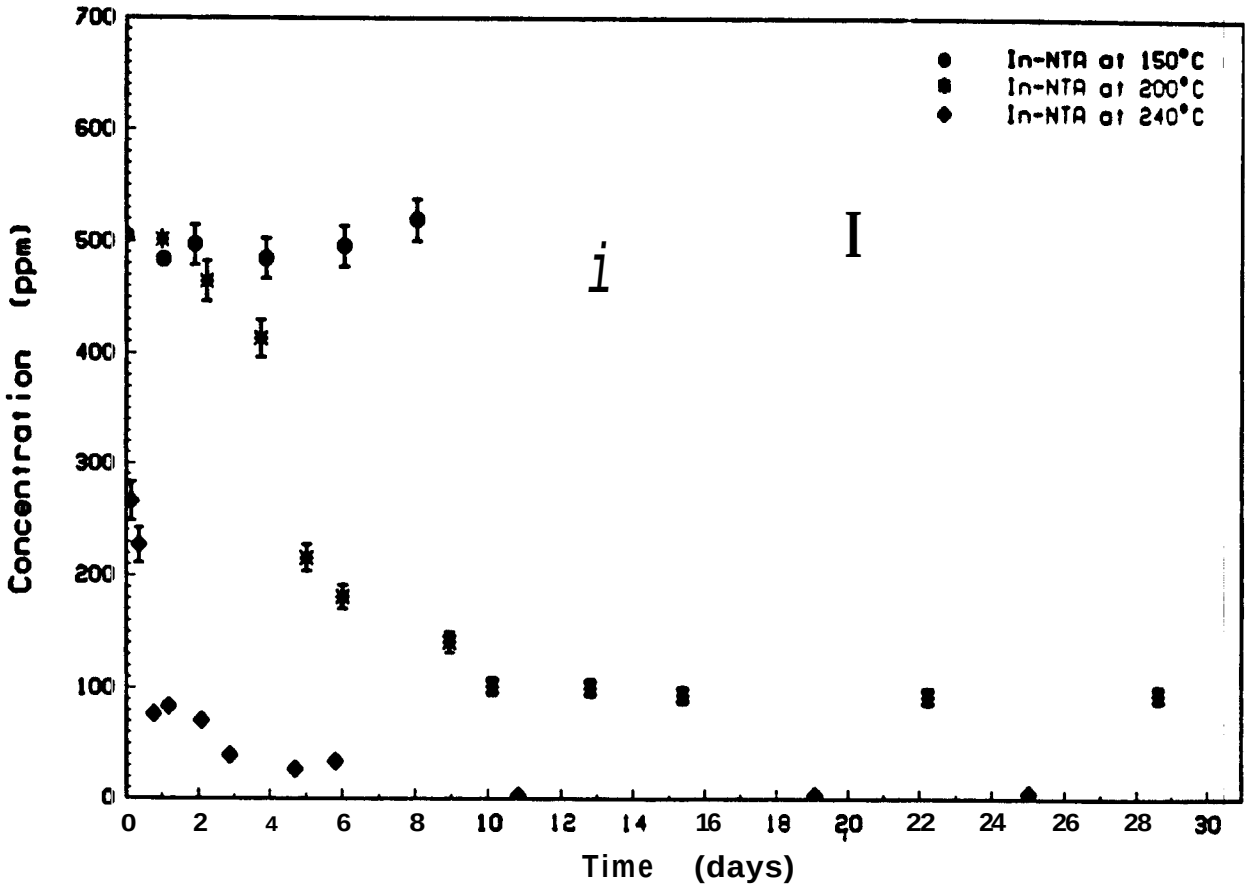

Fig. 3.4.2 Effect of temperature and time on **InNTA** stability.

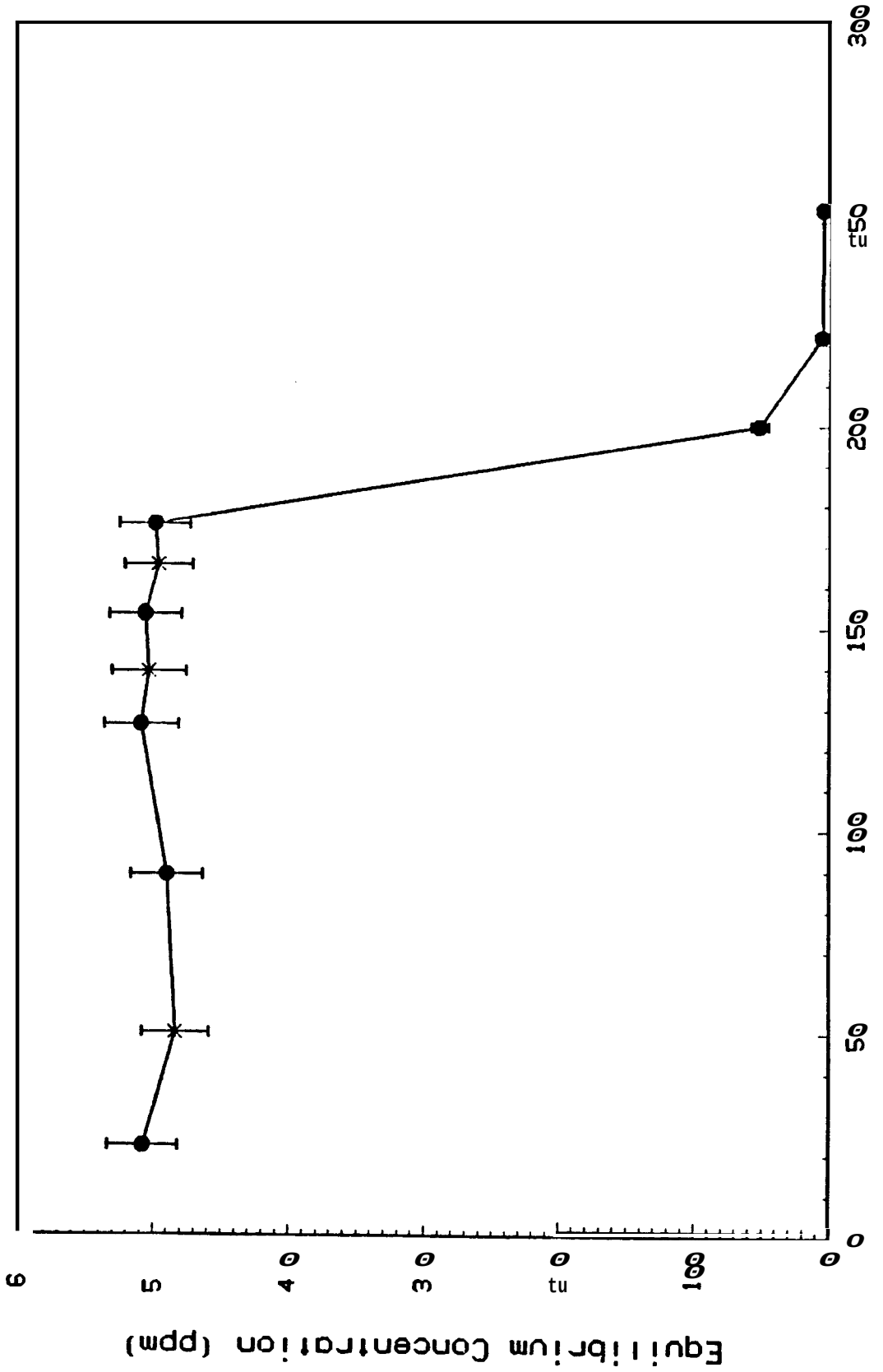

Fig. 3.4.3 Effect of T (°C) on InEDTA adsorption onto Graywacke sandstone.

The high cost of a large isotopic neutron source and regulatory restrictions on radioactive materials make this a difficult problem. Attention is also being given to the potential of the rare gases (chemically inert) Xenon and Krypton, in activable or stable form as clathrates, as useful high-sensitivity tracers for vapor-state fluids in vapor-dominated or two-phase geothermal reservoirs. The potential for such tracers is enhanced by their chemical inertness, low background in geothermal fluids, and sensitive methods for measurement, such as radiation spectroscopy and nuclear magnetic resonance.

* C. Chrysikopoulos and P. Kruger: "Thermal Stability of Chelated Indium Activable Tracers", Proceedings, 11th Annual Workshop on Geothermal Reservoir Engineering, SGP-TR-93, January, 1986.

** C. Chrysikopoulos, Engineering Degree Thesis, School of Engineering, Stanford University, 1986.

*** C. Chrysikopoulos and P. Kruger: "Chelated Indium Activable Tracer for Geothermal Reservoirs", SGP-TR-99, June, 1986.

4. FIELD APPLICATIONS

4.1 Cooperative Agreements

During the year, the Stanford Geothermal Program has had cooperative research, relationships with the Instituto de Investigaciones Electricas (IIE) in Mexico, ENEL in Italy, Ministry of Works and Development (MWD) in New Zealand, and Middle East Technical University (METU) in Turkey. For the most part, these cooperative programs are used as a means of field testing procedures developed either at Stanford or in cooperation with the other party. The individual tasks that have been undertaken are described in the sections of this report to which they pertain (for example, multiple well interference tests at Ohaaki are described in Section 2 and several heat sweep studies performed on Mexican fields are described in Section 3 of this report). During the current year, a number of additional projects were initiated between Stanford and its international partners. These will mostly be active during the coming year. Included in these are additional heat sweep studies at Los Azufres, La Primavera and Los Humeros fields, core analysis of Lardarello cores for adsorption effects, verification of tracer interpretation methods using two-dimensional flow models at METU.

In 1985, the Stanford Geothermal Program initiated a cooperative tracer test together with the New Zealand Ministry of Works and Development of Wairakei, New Zealand. The test involved a dual tracer test, first with injection of tracer into the Broadlands well BR23 and monitoring of the well BR20, followed by a second injection into BR20 and monitoring of BR23.

The objective of the test was to examine the premise that reinjected water travels through geothermal reservoirs in major conduits rather than in dispersed porous medium flow. If the flow were in a porous medium, it would be expected that the response of each of the two wells to injection in the other would be different, since hetero-

geneities over the area would disperse the tracer differently. On the other hand, if flow were in a major conduit, such as a fault or fracture, the response would be the same in both directions, even if the wells were not at the same depth.

The two tracer injections were performed by the New Zealand Institute of Nuclear Sciences in October 1985 and February 1986. The tracer used was radioactive Iodine-131. 69.5 GBq of 1-131 was injected into BR20 on October 17, 1985, and 55 GBq into BR23 on February 12, 1986. Good returns were found in both cases, although the *peak* arrival time of about 50 days was much longer than expected. Monitoring continued until **May** 1986.

Figure 4.1.1 shows the unprocessed tracer returns from the two tests. This data is still in the process of analysis, and has not been corrected for radiactive decay, or for the effect of recycling (fluid recovered from the production well was injected again into the reinjection well, thus carrying the tracer into the reservoir again).

This cooperative program has proved to be very worthwhile at very small expense to the Program. The expense of the field test and sample analyses was borne entirely by the Ministry of Works. The test satisfied the dual purpose of engineering analysis of reinjection in the field (which is soon to begin full-scale production), and scientific investigation. When the analysis of the data is complete, the test will provide data to help resolve some of the unanswered questions of how injected fluids move through geothermal reservoirs.

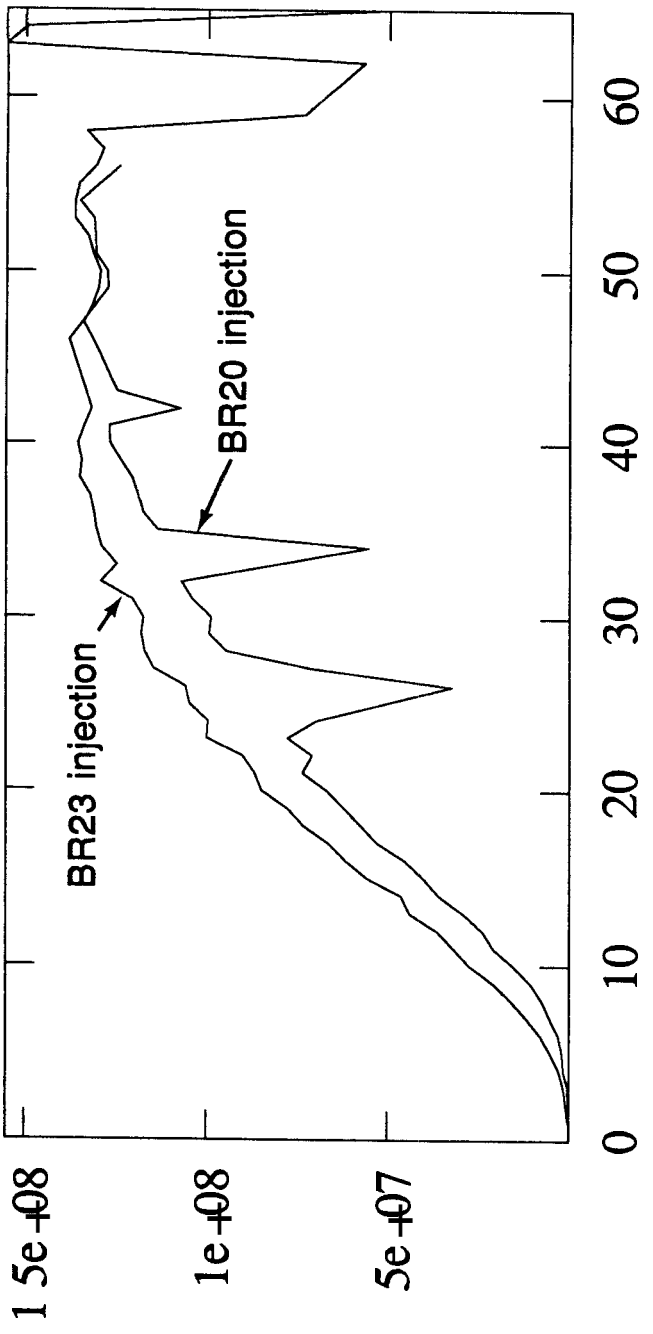

Fig. 4.1.1 Concentration profiles at production wells for the dual tracer test.

4.2 Use of the Hurst Simplified Method to History Match Field Performance

D. Brock and J. S. Gudmundsson

The applicability of the Hurst Simplified Method to model liquid-dominated geothermal reservoirs with recharge was studied. The model proved useful under the wide range of compressibilities found in such reservoirs.

Water influx methods in use fall into two categories: numerical and lumped parameter. Numerical models demand extensive data on reservoir and fluid characteristics, data which is not usually known for geothermal fields. Lumped parameter models are based on analytical solutions using average and constant characteristics and simple geometries.

The Hurst Simplified Method uses the Laplace transformation to yield an explicit expression for drawdown as an explicit function of time and production. Numerical methods are used to invert the Laplace solution when it is impossible to do so analytically.

A major difference in using the Hurst Method for geothermal applications (rather than petroleum reservoirs) is compressibility. Owing to the very high compressibility of two-phase (steam-water) zones that invariably occur in liquid-dominated geothermal reservoirs, the overall compressibility of such reservoirs can be three orders of magnitude greater than the compressibility of liquid water.

Thus, the Hurst Simplified Method was used to model sets of actual drawdowq data from five different geothermal fields covering a wide range of compressibilities! These were Ellidaar, Iceland (a small low-temperature field with little two-phase zones); Achuachapan, El Salvador; Wairakei, New Zealand; Svartsengi, Iceland; and Broadlands, New Zealand, a field known to have extensive two-phase zone.

Models of a field were done as follows (in the accompanying figures the Svartsengi field is used as an example). We are given a drawdown history, that is, a collection of data points of time, production rate, and drawdown. **A** model drawdown were calculated for the given production history and Hurst parameter (σ for the radial model, h, for the linear model). The model drawdown history is then compared to the actual drawdown history, and the standard deviation is calculated. the σ or h which minimizes the standard deviation is selected as the correct reservoir parameter. From the model, compressibility and k-h product are calculated. Predictions may also be done for a proposed production schedule. It was found that the Hurst model could match all the reservoirs tested, reservoirs spanning a range of compressibilities of almost three orders of magnitude. These matches are shown in Figures **4.2.1** through 4.2.5.

Thus, the Hurst Method model is usable on the wide range of compressibilities seen in liquid-dominated geothermal reservoirs. The model, through history matching, gives compressibility and k-h product. Further, the compressibility can be used to approximate the extent of two-phase zone in the reservoir. Comparing the matches using a linear model to those with a radial geometry gives insight into the geometry of the reservoir.

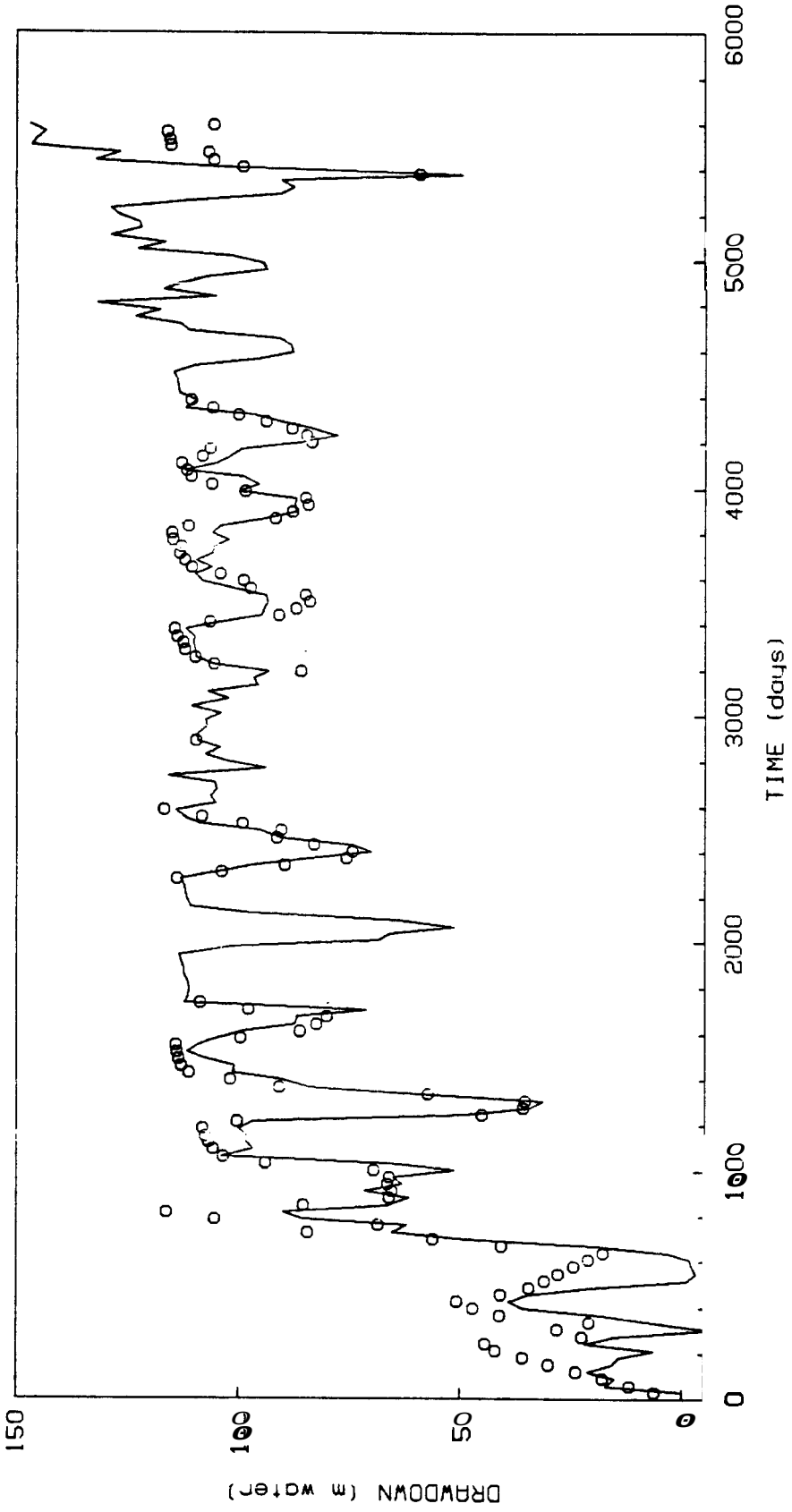

Fig. 4.2.1 Ellidar drawdown (radial line source model).

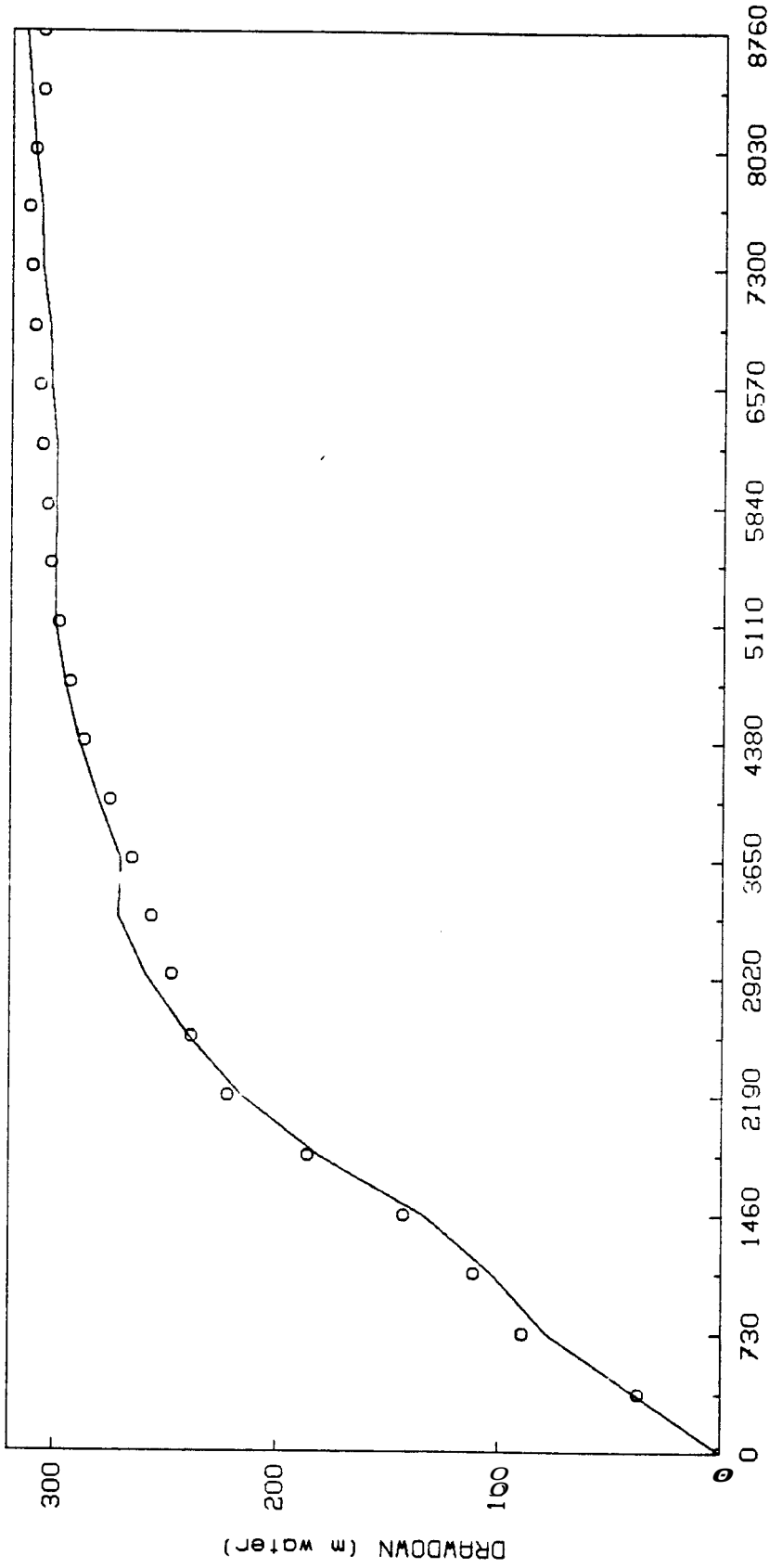

Fig. 4.2.2 Wairakei drawdown.

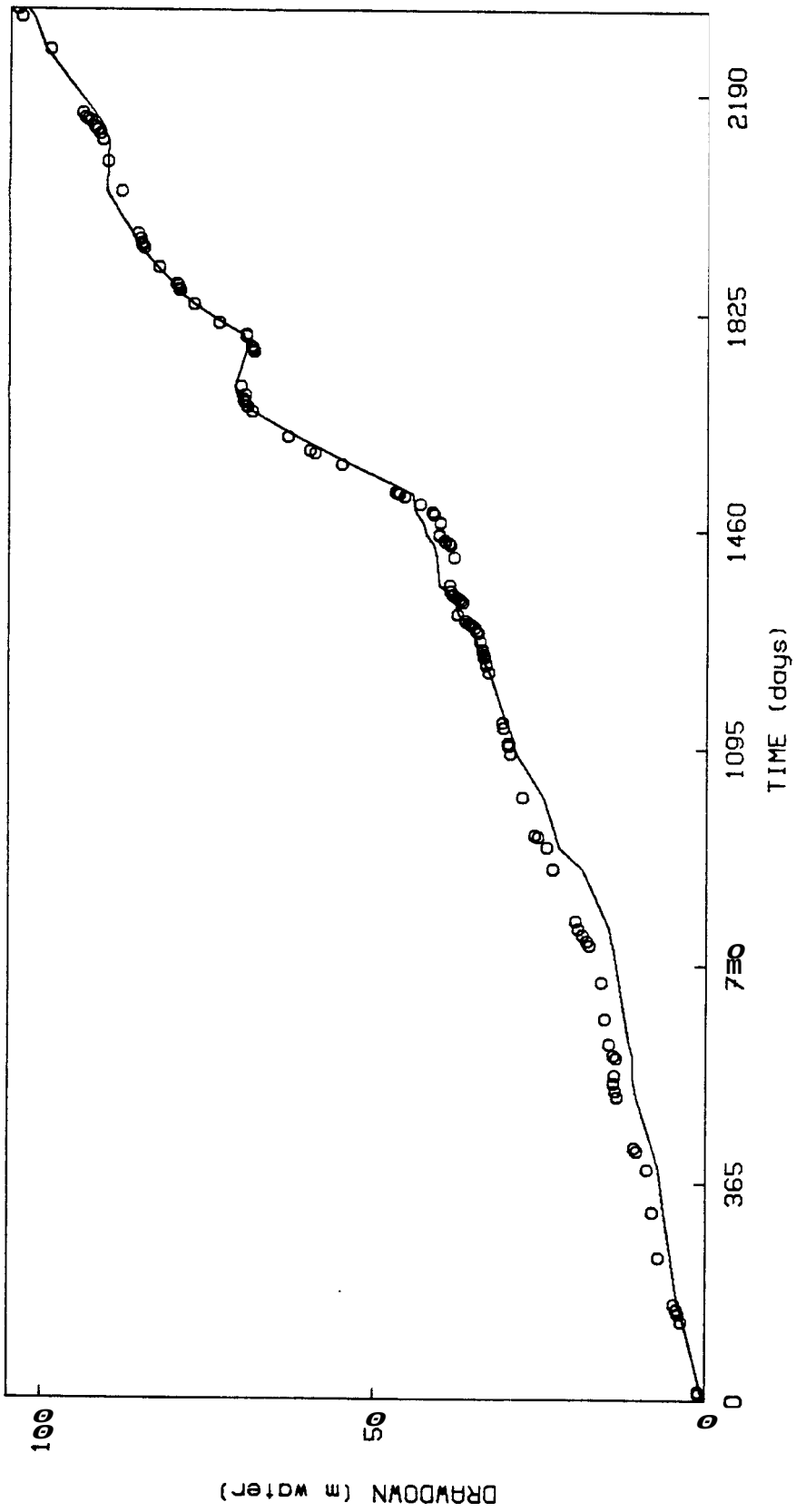

Fig. 4.2.3 Svartsengi drawdown.

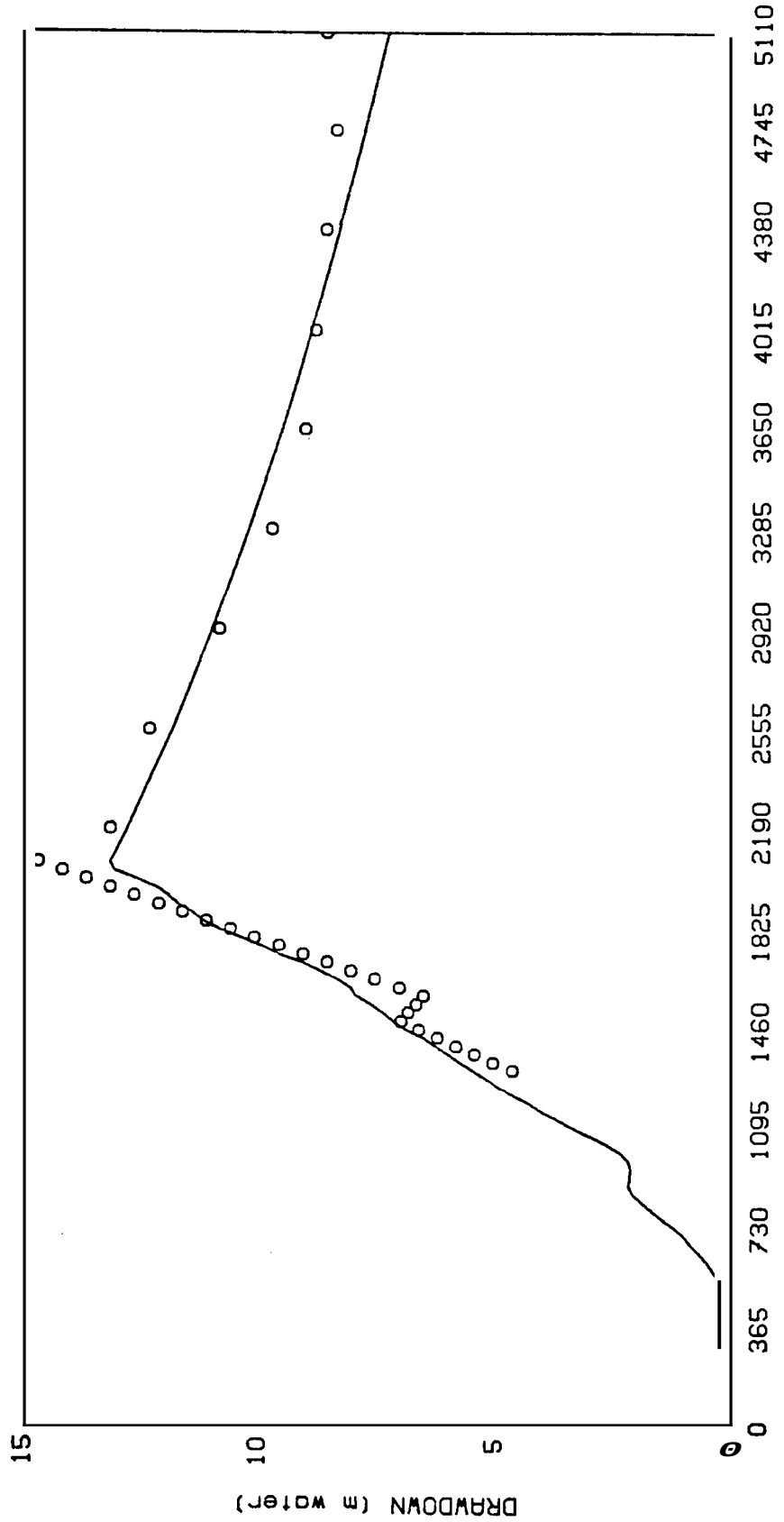

Fig. 4.2.4 Broadlands drawdown.

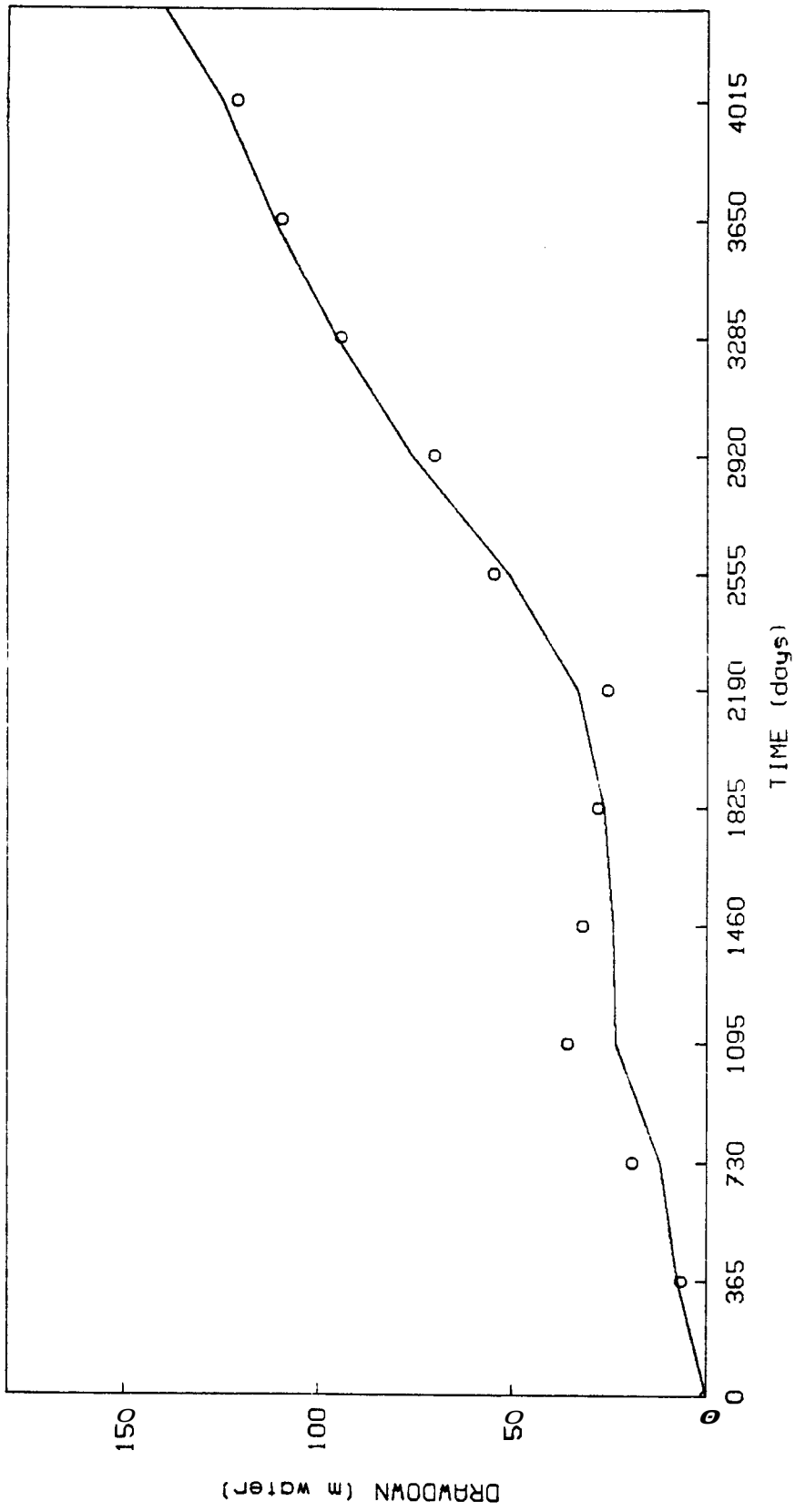

Fig. 4.2.5 Ahuachapan drawdown.

5. TECHNOLOGY TRANSFER

The Eleventh Workshop on Geothermal Reservoir Engineering was held at Stanford University on January **21-23, 1986.** The attendance was at the same level as tha previous year with about 144 registered participants. Ten foreign countries were represented: Canada, England, France, Iceland, Indonesia, Italy, Japan, Mexico, New Zealand and Turkey.

The purposes of the Workshop **are** to bring together researchers, engineers, and managers involved in geothermal reservoir studies and development, and to provide for prompt and open reporting of progress and the exchange of ideas. There were 38 technical presentations at the Workshop which were published as papers in the 11th Proceedings volume and one presentation was not published. Six technical papers not presented at the Workshop were also published in the Proceedings volume. In addition to these **45** technical presentations or papers, the introductory address was given by J. E. **Mock** from the Department of Energy.

Weekly seminars were held during the academic year on geothermal energy topics. Appendix A includes a list of the seminar topics for autumn, winter and spring quarters. These Seminars are attended by Stanford researchers and personnel of tha U.S. Geological Survey and geothermal companies in the San Francisco area. The seminars are also attended by representatives of geothermal companies in **Santa** Rosa.

Results of geothermal research at Stanford University were presented at several professional meetings during the year and issued. Appendix D includes a list of thesa publications and reports. The contents of the Proceedings of the Eleventh Workshop on Geothermal Reservoir Engineering are included in Appendix B.

APPENDIX A: Seminar Schedules

STANFORD GEOTHERMAL PROGRAM
STANFORD UNIVERSITY
STANFORD, CALIFORNIA 94305

Paul Kruger
Civil Engineering Dept.
Terman Bldg., Room M-19
(415) 497-4123 or 497-4744

SEMINAR SCHEDULE

Autumn Quarter 1985 — Room 124, Noble Building — Thursday, 1:15-2:30 p.m.

Date	Title	Speaker
Sept. 26	SGP Student Meeting	
Oct. 3	Tracer Dispersion Experiments	Roland N. Horne SGP
Oct. 10	Linear Boundary Detection in a Single Interference Test	Jonathan Leaver and Avrami Sageev SGP
Oct. 17	Application of the 1-D Linear Heat Sweep Model	Paul Kruger SGP
Oct. 24	Reservoir Testing	Henry J. Ramey, Jr SGP
Oct. 31	No Seminar IIE-SGP Joint Meeting	
Nov. 7	Hydrothermal Alterations in Geothermal Systems	Dennis Bird Geology
Nov. 14	Geological and Mineralogical Evaluation of Surface Geothermal Manifestations	Y. Yamaguchi and Ronald Lyon AES
Nov. 21	Study of Natural Fractured Systems with Digital Borehole Televiewer Analysis	Mark Zoback Geophysics
Nov. 28	Thanksgiving Recess	

STANFORD GEOTHERMAL PROGRAM
STANFORD UNIVERSITY

STANFORD, CALIFORNIA 94305

Paul Kruger
Civil Engineering Dept.
Terman Bldg., Room M-19
(415) 497-4123 or 497-4744

S E M I N A R S C H E D U L E

Winter Quarter 1986 — **Room 124, Noble Building** — **Thursday, 1:15-2:30 p.m.**

Date	Title	Speaker
Jan. 9	SGP Student Meeting	
Jan. 16	SGP Staff: Workshop Preparation	
Jan. 23	Eleventh Annual SGP Workshop (Jan. 21-23)	
Jan. 30	Review of Seventh NZ Workshop	Abraham Sageev, SGP
	Review of IIE-SGP Meeting	Frank G. Miller, SGP
Feb. 6	Geologic and Fluid-Flow Characteristics of the Cerro Prieto Geothermal Field	Susan Halfman, Lawrence Berkeley Lab.
Feb. 13	Update on Operations at The Geysers	Joel Robinson, Union Oil Company.
Feb. 20	Chevron Geothermal Activities in Nevada	Jerry Epperson, Chevron Resources
Feb. 27	Environmental Aspects of Power Generation at The Geysers	Ron Suess, PG&E
Mar. 6	Temperature Drop Model for Two-Phase Flow in Wellbores	Don Michels

STANFORD GEOTHERMAL PROGRAM
STANFORD UNIVERSITY

STANFORD, CALIFORNIA *94305*

John R. Counsil
Petroleum Eng. Dept.
Mitchell Bldg., Room 360
(415) 723-1218 or 723-4744

S E M I N A R S C H E D U L E

Spring Quarter 1986 — **Room 124, Noble Building** — **Thursday, 1:15-2:30 p.m.**

Date	Title	Speaker
April 10	Organizational Meeting	SGP Faculty
April 17	No Seminar (Affiliates Meeting)	
April 24	Use of the Hurst Simplified Method to History Match the Performance of Five Geothermal Fields	Dave Brock Petroleum Engineeking
May 1	Injection Tracer Backflow Tests	Ibrahim Kocabas Petroleum Engineeking
May 8	Tracer Dispersivity in Fractures	Larry Bouett Petroleum Engineeking
May 15	Linear Skin Boundaries	Anil Ambastha Abraham Sageev Petroleum Engineering
May 22	Adsorption of Steam on Geothermal Cores	Jeralvn Luetkehans Paul Pettit Petroleum Engineering
May 29	Computer Generation of Type Curves Interference Testing w th Boundaries	Brenna Surritt Abraham Sageev Petroleum Engineering

APPENDIX B: Table of Contents Proceedings Eleventh Workshop

TABLE OF CONTENTS

Modeling

Geosciences

Discussion on Maturing Geothermal Fields

Field Studier

Logging

• This work is available as a Stanford University, Department of Geology Master's Report, "Solution Mineral Equilibria in the Coro Geothermal Syrtem," B. Bishop, 1983.

APPENDIX C: Participants in the Stanford Geothermal Program

Faculty	Reservoir Technology Research Assistants (and others)
Henry J. Ramey, Jr.	Dave Brock
Paul Kruger	James W. Lovekin
Roland N. Horne	Jeralyn Luetkehans
Frank G. Miller	Tom Lyons
William E. Brigham	Steve Lamb
Abraham Sageev	Beatriz Salas
John Counsil	Anil Ambastha
	Costos Chrysikopoulos

APPENDIX D: Papers Presented and Published 1985-86

1. Barua, J., Horne, R. N., Greenstadt, J. L., and Lopez, L.: "Improved Estimation Algorithms for Automated Type Curve Analysis of Well Tests", paper SPE 14255, Proceedings, 1985 SPE Annual Conference and Exhibition, Las Vegas, NV, Sept. 23-25, 1985.
2. Gerard, M. G., and Home, R. N.: "Effects of External Boundaries on the Recognition and Procedure for Location of Reservoir Pinchout Boundaries by Pressure Transient Analysis", Soc. Pet. Eng. J., June 1985, 427-436.
3. Home, R. N., and Kucuk, F.: "The Use of Simultaneous Spinner and Pressure Measurements to Replace Isochronal Gas Well Tests", paper SPE 14494, Proceedings, SPE Eastern Regional Meeting, Morgantown, Virginia, Nov. 6-84 1985.
4. Horne, R. N., Gilardi, J. R., and Bouett, L. W.: "Dispersion of Tracers in Fractures", Proceedings, 7th New Zealand Geothermal Workshop, Auckland, New Zealand, 1985, p. 61-64.
5. Sageev, A., and Home, R. N.: "Interference Between Constant Rate and Constant Pressure Reservoirs Sharing a Common Aquifer", SPE Journal, June 1985, 419-426.
6. Walkup, G. W., Jr.. and Horne, R. N.: "Forecasting Thermal Breakthrough of Reinjected Water Using a Dispersion-Retention Model for Tracer Test Interpretation", GRC Transactions, 9, part II, August 1985, p. 369-374.
7. Dye, L. W., Horne, R. N., and Aziz, K.: "A New Method for Automated History Matching of Reservoir Simulators", paper SPE 15137, Proceedings, 1986 SPE California Regional Meeting, Oakland, CA, April 2-4, 1986, 443-461.
8. Home, R. N., Perrick, J. L., and Barua, J.: "Well Test Data Acquisition an Analysis Using Microcomputer", paper SPE 15308, Proceedings, SPE Symposium on Petroleum Industry Applications of Microcomputers, Silver Creek, CO, June 18-20, 1986.
9. Leaver, J. D., and Sageev, A., and H. J. Ramey, Jr.: "Multiple Well Interference Testing in the Ohaaki Geothermal Field', SPE 15112, presented at the California Regional Meeting, SPE of AIME, Oakland, CA, 1986.
10. Masukawa, J., and Horne, R. N.: "The Application of the Boundary Integral Method to Immiscible Displacement Problems", paper SPE 15136, Proceedings, 1986 SPE California Regional Meeting, Oakland, CA, April 2-4, 1986, 433-442.
11. Menninger, W., and Sageev, A.: "Breakthrough Time for the Source-Sink Well Doublet", presented at the 11th Workshop on Geothermal Reservoir Engineering, Stanford, CA, 1986.
12. Pulskamp, J. F., Johns, R. A., and Horne, R. N.: "Experimental Tracer Response Curves for Fractured Cores", GRC Transactions, 10, 1986.

13. Sageev, A.: "Slug Test Analysis", Water Resources Research Journal, Vol. 22, No. 8, 1323-1333, 1986.

14. Sageev, A., and Home, R. N.: "Interference Testing: Detecting an Impermeable or Compressible Region", paper SPE 15585, Proceedings, 1986 SPE Annual Conference and Exhibition, New Orleans, LA, Oct. 5-8, 1986.

15. Sageev, A., and H. J. Ramey, Jr.: "On Slug Test Analysis in Double-Porosity Reservoirs", SPE 15479, presented at the Annual Technical Conference and Exhibition, SPE of AIME, New Orleans, LA, 1986.

16. Sageev, A., Leaver, J. D., and H. J. Ramey, Jr.: "The Significance of Early Time Data in Interference Testing for Linear Boundary Detection", presented at the 1lth Workshop on Geothermal Reservoir Engineering, Stanford, CA, 1986.